Univerzita Karlova
Přírodovědecká fakulta

Studijní program: Chemie

Studijní obor: Chemie

Martin Orságh

Systémová chemie: logická hradla založená na sol-gel přechodech arylboronových kyselin

Systems chemistry: logic gates based on the stimuli-responsive sol-gel transition of arylboronic acids

Bakalářská práce

Školitel: Ing. Mariusz Marcin Uchman, Ph.D.
Konzultant: doc. RNDr. Pavel Matějíček, Ph.D.

Praha, 2021

Prohlášení:

Prohlašuji, že jsem závěrečnou práci zpracoval samostatně a že jsem uvedl všechny použité informační zdroje a literaturu. Tato práce ani její podstatná část nebyla předložena k získání jiného nebo stejného akademického titulu.

V Praze, 17. 6. 2021   ....

Abstrakt

Gelátory jsou látky schopny tvorby gelů, zahřňajíc podskupinu hydrogelů, materiálů s jedinečnými viskoelastickými vlastnostmi, kde je kapalnou složkou voda. Hydrogely jsou běžně používané v zemědělství a jsou aktivně zkoumány pro potenciální bioaplikace, ku příkladu v oblastech tkáňového inženýrství nebo jako nosiče léčivých přípravků s řízeným uvolňováním. Nicméně, takové aplikace vyžadují hlubší poznání struktury a biokompatibility takových gelátorů. Přesto že je známo mnoho tříd gelátorů s nízkou molekulovou hmotností, variace v jejich struktuře mají nepředvídatelné následky na jejich schopnost tvořit gel. V tomto kontextu naše skupina objevila nový gelátor s nízkou molekulovou hmotností, kyselinu 3-izobutoxyfenylboronovou (PBA), s jedinečnou strukturou, schopnou gelace vody při velmi nízkých koncentracích. K analýze struktury, mechanických vlastností a jejich závislostí na teplotě jsme využili reometrii, elektronovou mikroskopii a diferenciální skenovací kalorimetrie. Dále jsme studovali efekt močoviny na viskoelastické vlastnosti tohoto gelu a reaktivitu gelu vůči chemickým stimulem (jako například změna pH, přidání diolů nebo jiných biochemicky relevantních látek), kterou jsme interpretovali v termínech logických bran. Naše výsledky prezentují praktičnost PBA jako gelátoru, jehož viskoelastické vlastnosti a teplota sol-gel přechodu jsou nastavitelné koncentrací gelátoru případně přídavkem močoviny.

Abstract

Gelators are compounds capable of producing gels, including hydrogels, materials with unique viscoelastic properties whose liquid component is water. Hydrogels are already commonly used in agriculture and currently tested for potential bioapplications such as scaffolds in tissue engineering and even as carriers in drug delivery. However, such applications require deepening our knowledge of assembly, structure and biocompatibility of gelators. Although many known classes of low-molecular-weight (LMW) gelators are already available, structural variations have highly unpredictable consequences on their gelating abilities. In this context, our group has discovered new LMW gelator, 3-isobutoxyphenylboronic acid (PBA), with unique structure, capable of gelating water at low concentrations. To analyze its mechanical properties and their variation as function of temperature we used rheometry, electron microscopy and differential scanning calorimetry. We also assessed the effect of urea on the viscoelastic properties of hydrogels gelated by PBA to test the tunability of viscoelastic properties of these gels. In addition, we studied the ability of PBA to react by sol-gel transition to external stimuli, such as changes in pH or composition (by adding diols or other biochemically relevant compounds). Hybrid urea-doped PBA hydrogel reactive to urease was made. Based on these reactions, we were able to construct functional and simple logic gates with sol-gel response. Our results highlight the versatility of PBA as a gelator, whose viscoelastic properties and gelation temperature can be tuned by changing its concentration and by addition of urea. Ultimately, these findings may enable us to use tissue scaffolding regulated by external addition of urea to control stem cell differentiation.

Abbreviations

4-MMBA - 4-methoxyphenylboronic acid

AFM - atomic force microscopy

ATP - adenosine triphosphate

CMOS - complementary metal-oxide semiconductor

COF - covalent organic framework

DSC - differential scanning calorimetry

EM - electron microscopy

FFT - fast Fourier transformation

GST - glutathione S-transferase

HRTEM - high resolution transmission electron microscopy

LMW - low molecular weight

NMR - nuclear magnetic resonance

PBA - 3-isobutoxyphenylboronic acid

SAXS - small angle x-ray scattering

SEM - scanning electron microscopy

TEM - transmission electron microscopy

UV - ultraviolet

WAXS - wide angle x-ray scattering

Table of contents

1. Overview

Hydrogels consist of major liquid (water) and minor solid (gelator) components with intermediate viscoelastic properties between solid and liquid and with a wide range of applications, particularly in biomedicine, thanks to their biocompatibility.[1] Among these applications, their potential uses as scaffolds in tissue engineering and as carriers in drug delivery stand out for their ability to provide structural support for cell division while mimicking real tissue[2] and to respond to external stimuli when releasing a drug[3] respectively. Accordingly, these applications depend on the physical and chemical properties of the gelator and on its biocompatibility.

Low-molecular-weight (LMW) gelators, in particular, are capable of easily triggered reversible gelation because they are composed of small organic molecules bound by non-covalent interactions.[4] In addition, LMW gelators are more easily biodegraded and often more biocompatible than most classical polymer gelators. Most LMW gelators share a common framework design with small structural alterations specifically introduced to generate molecular responsive properties, including responsiveness to light, temperature, magnetic fields and chemical stimuli.[5] However, this approach is limited by the sensitivity of LMW gelators to structural changes, whereby extremely small changes, such as introducing a single functional group, can preclude their ability to gelate. One of commonly used functionalization consists of introducing arylboronic acid into a gelator structure.

Arylboronic acids are widely known for their ability to interact with 1,2- and 1,3-diols, which are abundantly found in many biochemically relevant compounds such as sugars, glycosides, or even some hormones.[6] This reactivity has been well studied from a chemical point of view and is now being studied for possible pharmaceutical applications, such as stimuli-triggered drug delivery. In addition to their reactivity to diols, arylboronic acids are also responsive to changes in pH, anion concentration and presence of amines. This wide range of reactivities is very interesting not only for drug-delivery and sensing purposes, but also for its possible implementation in molecular logic gates. Interesting point of view on reactivity of particular compound can be gained by studying its properties as molecular logic gate. By smart definition of physical inputs, one can look at complex chemistry of the compound (and its systems) in more mathematical and analytical way using Boolean algebra.

Our lab is specialized in studying of arylboronic acids self-assembly and their reactivity (particularly polymers modified by arylboronic acid functionalization as smart responsive materials[7,8,9,10]) and their drug-delivery applications.

In this thesis we characterized its thermodynamic and viscoelastic properties and sol-gel transition reactivity to chemical stimuli. Furthermore, we characterized the microscopic structure of our newly discovered hydrogel by scanning electron (SEM), high resolution tunneling electron microscopy (HRTEM) and atomic force microscopy (AFM). We also preliminarily investigated the molecular assembly that lead to such gels using x-ray diffraction methods such as SAXS and WAXS and experimentally assessed the effects of various chemical stimuli on the sol-gel transition, interpreting the results in terms of logic gates. We further evaluated the effect of urea (a key biological compound and chaotropic agent) on sol-gel transition temperatures and viscoelastic properties. Because PBA is such a simple compound with only one boronic functional group, we must use various chemical systems capable of inducing either pH changes or pH-dependent diol binding. As such, we considerably simplified pH/diol AND gate, and produced other basic logical gates such as OR, NOR, NAND and IMPLY gates and further studied the responsiveness of our gelator to pH changes caused by urease, a common enzyme produced by many pathogenic bacteria.

2. State of the art

2.1. Chemistry of arylboronic acids

Arylboronic acids are organic compounds consisting of benzene ring substituted with $B(OH)_2$ group. They are mostly known because of their applications in organic synthesis, mostly aryl coupling reactions. They are easily accessible from aryl halides by Miyaura borylation reaction[11] (Scheme 1) and most simple arylboronic acids are sold as building blocks for synthesis. Probably most well known aryl-aryl coupling reaction, Suzuki coupling, utilize palladium catalyzed reaction of aryl halide with arylboronic acid to produce corresponding biaryl[12] (Scheme 2). Besides extreme popularity of arylboronic acids in organic chemistry they are also widely studied as potential molecular sensors, drug-delivery mechanisms and even special applications such as boron neutron capture therapy.[13]
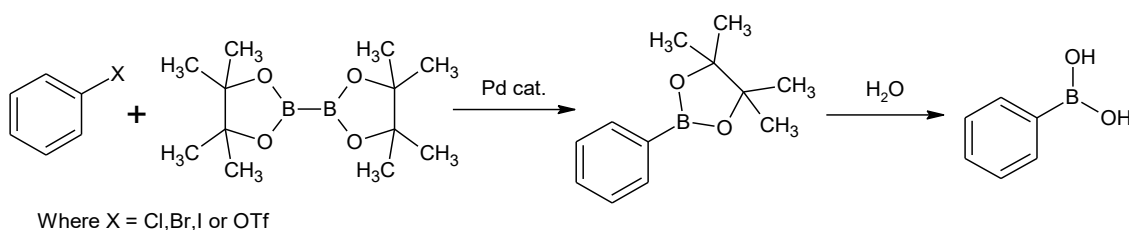
Scheme 1: Miyaura borylation with subsequent deprotection of arylboronic acid
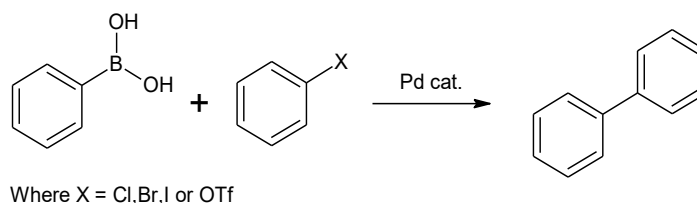
Scheme 2: Simplified scheme of Suzuki coupling

Because of boron capability of accepting electron pair and its decreased electron density by two hydroxyl groups, arylboronic acids are capable of reacting with hydroxide anion to produce arylboronate anion, therefore they are considered as a Lewis acid. Acidity of arylboronic acids can be easily tuned by substitutions on benzene ring, for example pK_a ranging from 9.24 for *p*-methoxy substituted phenylboronic acid, up to 7.23 for *p*-nitro substitution.[14] In special cases when substituent is able to stabilize tetrahedral boronate anion structure such as 2-(N,N-dimethylaminomethyl)phenylboronic acid (also known as Wulff type) where nitrogen coordinates boron, pK_a as low as 5.3 can be achieved.[15] Other possibility is swapping nitrogen with oxygen leading to benzoxaborole structure with $pK_a = 7.5$, which is actually quite close to physiological pH.[15] pK_a values close to physiological pH are highly desired for drug-delivery purposes and molecular sensors.

Arylboronic acids are also well known to undergo dehydration to form cyclic trimers (boroxines). This unusually simple and easily reversible trimerization (in combination with wide range of other interesting reactions) has been extensively studied for applications in covalent organic frameworks (COF).[16]

Functionalization of various drug delivery mechanisms such as micelles, liposomes, or even gels with arylboronic acid precisely tuned for reactivity towards saccharides at physiological pH is very attractive for insulin-release mechanisms. Such systems are already extensively studied and

have already shown extremely promising results for treatment of diabetes.[17] Interesting particular case of copolymer of lactic and glycolic acid modified with arylboronic acid has shown extremely low cytotoxicity in *in vitro* assays and capability of maintaining normal insulin levels in induced diabetic mouse model in *in vivo* assays for up to 2 weeks.[18]

Interesting aspect of arylboronic acids is their reactivity towards 1,2- or 1,3-diols, which are common structural part of many important biomolecules (sugars, glycosides, hormones etc.). In aqueous solutions addition of such diol leads to equilibrium of arylboronic acid, its anion, and arylboronate ester and corresponding anion (Scheme 3). Because of this complex equilibrium, presence of diols in aqueous solution of arylboronic acid can lead to changes in apparent pK_a.

Arylboronic esters are stronger acids than free arylboronic acids so in most cases apparent pK_a is lowered. As an example, Marinaro et al.[19] determined these constants for 4-methoxyphenylboronic acid (4-MMBA) and a few other boronic acids by potentiometric titration. For 4-MMBA the reported acidities are $pK_{a1} = 9.32$ and $pK_{a2} = 6.25$, more than 1000-fold higher acidity constant. Ester equilibrium constants (K_{B1} and K_{B2}) are dependent on studied alcohols, in example constants for ethylene glycol are $K_{B1} = 2.8 \cdot 10^{-3}$ and $K_{B2} = 2.6$, while equilibrium constants for glycerol are much higher: $K_{B1} = 4.5 \cdot 10^{-2}$ and $K_{B2} = 41.5$ (this is caused because ethylene glycol is diol and glycerol is triol and also glycerol is capable of 1,2-diol interaction and also 1,3-diol interaction). Reactivity towards diols has been extensively studied[6] for sensing of glucose, fructose or dopamine.
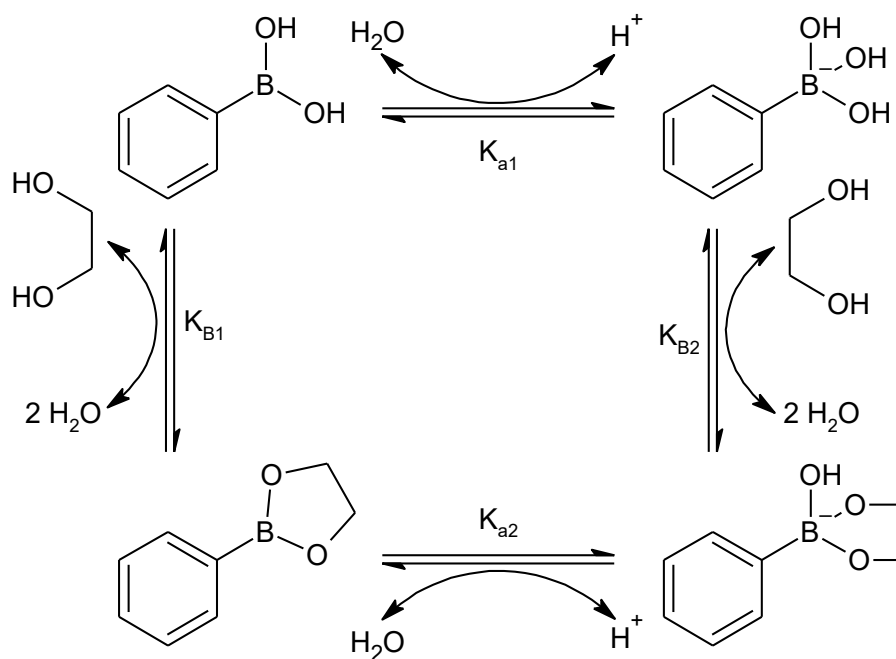
Scheme 3: Complex equilibrium of phenylboronic acid with ethylene glycol in water

Because of two OH groups, arylboronic acids are considered slightly hydrophilic, without substitution with other hydrophilic groups most of them are very slightly soluble in water at room temperature, although at higher pH by coordination of hydroxide anion, or after coordination of i.e. fluoride, their anionic form is prevalent in aqueous solution, which as charged functional group is highly hydrophilic.

Coordination of fluoride to arylboronic acids has been studied as fluorescent indicator of fluoride, common toxin causing dental fluorosis. In the case of fluoride sensor utilizing fluorescent

indication,[20] coordination of fluoride on arylboronic acid in combination with pyridinium part of molecule lead to zwitterion which is able to aggregate from solution. Because of pyrenyl substitution, aggregates are highly fluorescent. These properties combined with effect of 1,2- or 1,3- diols predicts interesting properties for molecular recognition. Other major interactions of arylboronic acids are hydrogen bonding of OH groups, which can be commonly seen as dimerization in crystal structure of arylboronic acids (similar to that in Figure 1), and hydrophobic interactions, mostly π-stacking of aryl-rings, which is characteristic for unhindered arylboronic acids.[21]
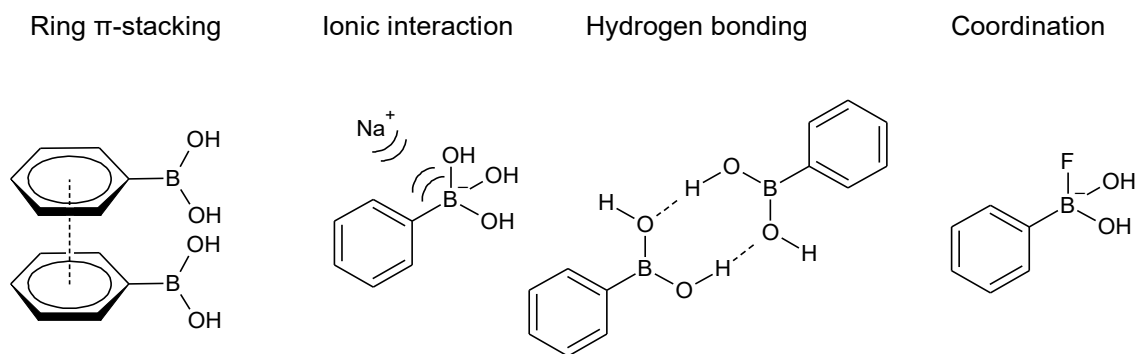
Figure 1: Common interactions characteristic for arylboronic acids

2.2. Hydrogels design and applications

Gels are two component systems composed of minor (solid) gelator and major liquid component. Hydrogels are special cases of gels, where liquid component of gel is water or aqueous solution (in contrast to organogels where liquid phase is organic solvent). These type of gels are especially interesting, because of wide field of applications, ranging from simple absorbent napkins and diapers to biomedical applications such as contact lenses pioneered by Wichterle in 1960 which are still commonly used today.[22]

Hydrogels can be divided into two main groups, chemical and physical hydrogels. Chemical gels are cases of gelator being covalently bonded network, often largely crosslinked polymers, which leads to robust but irreversible gel. On the other side, in case of physical gels, gelator is often small polymer, or even relatively small molecule, holding together by noncovalent interactions (such as hydrogen bonding, π-stacking and many others) creating network structure. These types of gels are considered reversible as they are able to be reliquefied, often by simple heating. Xerogels can be produced by carefully drying of gel without mechanically disturbing its solid component, leaving solid network of gelator.

Special case of gelators are low molecular weight gelators, in which small molecules interact noncovalently to produce 3D network of gel. Structures of LMW gelators are extremely variable, in many cases we can describe amphiphilic architecture, although there are exceptions. In case of hydrogels, non-polar part is often composed of aromatic rings or long alkane chain. Polar part can be highly variable, common groups are amino acids or oligopeptides, carbohydrates or so called gemini surfactants which can be described as two surfactant molecules (charged head and long alkyl tail) linked at polar part with short linker.[23] Overall LMW gelators are compounds that can be described as capable of preferential one-dimensional aggregation leading to network of gel.[24]
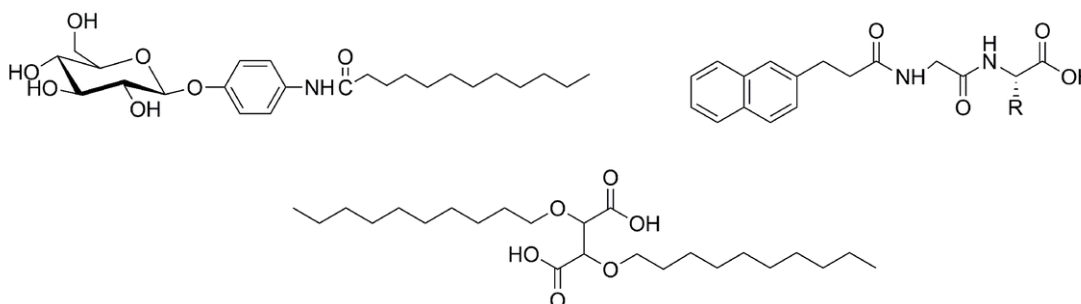

Figure 2: Examples of LMW gelators: carbohydrate based (top-left), oligopeptide based (top-right), gemini surfactant (bottom) [23]

Hydrogels can be also utilized as sensors. Modification of gelator with functional group reactive to certain stimuli can produce gel sensitive to that stimuli with sol-gel phase transition response (in the case of LMW gelators one must pay attention that even small changes such as one functional group can cause compound to be able to crystallize or dramatically change solubility to extent of losing gelator behavior). Nice example of such modification providing stimuli sensitivity is tripeptide based LMW gelator, where the tripeptide tail is substituted with 4-(hydroxymethyl)-phenylboronic acid (Figure 3.A).[25] Esters of 4-(hydroxymethyl)-phenylboronic acid are capable of being cleaved by peroxide. Such structural change leads to irreversible destabilization of gel nanofibers, therefore causing collapse of gel. Sensitivity towards peroxide is useful indicator of oxidase activity (many oxidases produce hydrogen peroxide as side product).

Arylboronic acid modified gelators are no exceptions to designs mentioned above. In Figure 3 we can clearly distinguish "traditional" amphiphilic architecture consisting of hydrophilic head and hydrophobic tail. This can be better shown on the case of gelator in Figure 3.C, composed of

hydrophilic arylboronic acid substituted with carbamate group and hydrophobic cholesterol tail, similarly Figure 3.B is utilizing glutamate esterified by hydrophobic fatty alcohols. In case of molecular logic gate in Figure 3.A similar situation can be observed. Although oligopeptide tail is often considered hydrophilic, this is compensated by use of hydrophobic amino acids, such as phenylalanine.
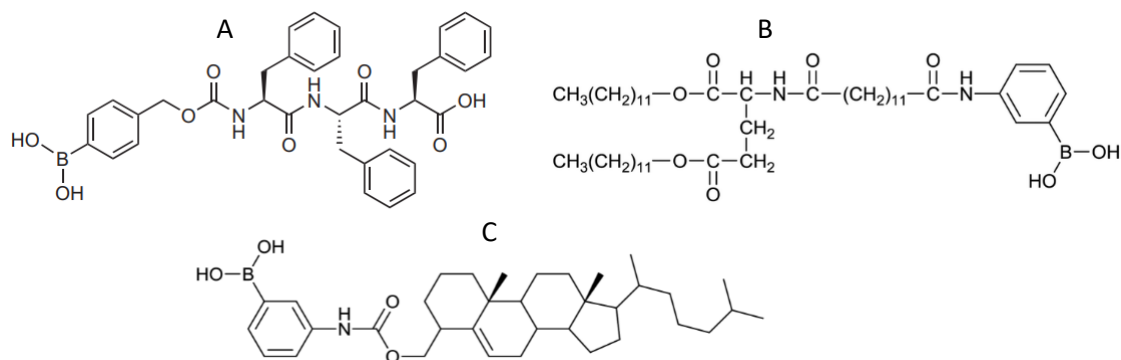

Figure 3: Examples of arylboronic acid based LMW gelators[26]

It has been shown, that utilizing known design with possible tuning of viscoelastic properties, differentiation of mesenchymal stem cells in *in vitro* experiments can be altered by changes in elastic properties of hydrogel[27] by changing side-alkyl chain length. This research also proves that stem cells differentiation can be regulated by mechanical properties, even in absence of biochemical stimuli. Choice of LMW gelator in this case is very promising, not only because of their biocompatibility but also because of their easily tunable viscoelastic properties.

From the rheology point of view, gel can be classified neither as a liquid nor solid because of its unique viscoelastic properties, more accurate description would be somewhere in between. Old definition of gel in IUPAC goldbook[28] has been based on finite and rather small yield stress. This means that gel is behaving as elastic solid under quite small forces, but it is easy to get beyond yield point after which part of force will cause non-reversible deformation. For chemical gels interesting characteristics is often storage and shear loss moduli dependence on time, time of some chemical reaction (i.e. crosslinking) changing physical properties of gel. In case of physical gels with rapid phase transition more interesting characteristics are storage and shear loss moduli dependence on temperature. Furthermore, when studying physical gels by rheology, care must be taken to apply only small deformation when studying sample, to avoid perturbing of gelation process.

2.3. Logic gates

Logic gates are systems capable of performing logical operation on binary inputs. They are basic building block of any electronical computational device used today. Discovery of first practical electronical logic gates composed of vacuum tubes, meant start of technological revolution.[29] This was followed by discovery of transistors and integrated circuits capable of shrinking sizes of logic gates to sub-millimeter sizes, resulting to 1969 when man landed on the Moon controlled and navigated by computer composed solely of integrated circuits with only NOR gates.[30]

Most common and basic 2-input logic gates (Table 1, inputs are represented as A and B, with output X), often used in electronics are:

- OR gate performs logical disjunction, logical output is true if any of the inputs is true.
- AND gate performs logical conjunction, both of the inputs have to be true for output to be true. If only one or neither of inputs are true, output is false.
- NOT gate performs logical negation, therefore if input is false, output will be true and vice versa.
- IMPLY gate performs logical conditional, the only case when output is false is when first input is true and second false. Combination of first input false and second input true lead to output being true.
- NAND gate can be described as logical negation of output of AND gate
- OR gate can be described as logical negation of output of OR gate

Important aspect of NAND and NOR gate is functional completeness, meaning any logical operation can be performed by a set of connected NAND, or NOR gates respectively.

Name	NOT	AND	NAND	OR	NOR	XOR	XNOR
Alg. Expr.	$\overline{A}$	AB	$\overline{AB}$	$A+B$	$\overline{A+B}$	$A \oplus B$	$\overline{A \oplus B}$
Symbol							

Truth Table	A	X	B	A	X	B	A	X	B	A	X	B	A	X	B	A	X	B	A	X
	0	1	0	0	0	0	0	1	0	0	0	0	0	1	0	0	0	0	0	1
	1	0	0	1	0	0	1	1	0	1	1	0	1	0	0	1	1	0	1	0
			1	0	0	1	0	1	1	0	1	1	0	0	1	0	1	1	0	0
			1	1	1	1	1	0	1	1	1	1	1	0	1	1	0	1	1	1

Table 1: Most common logic gates and their respective truth tables[31]

2.3.1. Molecular logic gates

When implementing logic gates in chemical systems, care has to be taken that inputs of traditional logic gates are binary, either 1 or 0 (true or false respectively). Therefore we have to define input not only as compound but also as amount leading to positive input. This could seem counterintuitive, but the same has to be done for example with voltage on transistors, where we have to define threshold voltage. In molecular logic gates the binary inputs are often performed by presence or absence of certain compound (presence of ions, change in pH) or presence or absence of light of certain wavelength. Binary outputs are often simple physical phenomena such as change of color, change in fluorescence spectra or phase transition.

One of the reasons to study molecular logic gates is that it forces us to look on complex reactivity of particular chemical compound in different way. Chemical equivalent of OR gate can be interpreted as compound being reactive to either of compounds without interference. Equivalent of AND gate is that presence of both reagents is needed for response, this can mean for example that certain reaction or interaction is happening between the two inputs (either mediated or not, by the gate itself) leading to response. By studying simple molecular logic gates and creating such "libraries" of known reactions leading to molecular response, with possibly very little concentration dependence, one can apply this to more complicated systems.

Difference between input and output causes that these molecular logic gates are not easily connectable and therefore not very useful for computational tasks compared to their electrical siblings (although similar simplified systems have been discovered utilizing oscillatory reaction).[32] However, direct reaction to chemical input can be useful for example, in analytical chemistry (identification of presence or absence of given combination of analytes).

Another even more interesting possibility is directed therapy, such as molecular logic gate TOPI-4,[33] which activity can be seen in Figure 4, where glutathione S-transferase (GST) is inhibited by molecular logic gate TOPI only in absence of beta-cyclodextrin, and TOPI-4 is strongly fluorescent only in presence of glutathione S-transferase and absence of cyclodextrin, behaving as molecular INHIBIT gate. By modulating activity of glutathione S-transferase TOPI has effect on cell viability and has been demonstrated to lower cancer cell overexpressing glutathione S-transferase viability much better in absence of cyclodextrin „antidote". Adamantanecarboxylic acid (Ad-COOH) can competitively bind to cyclodextrin and activate TOPI-4 inactivated by cyclodextrin.
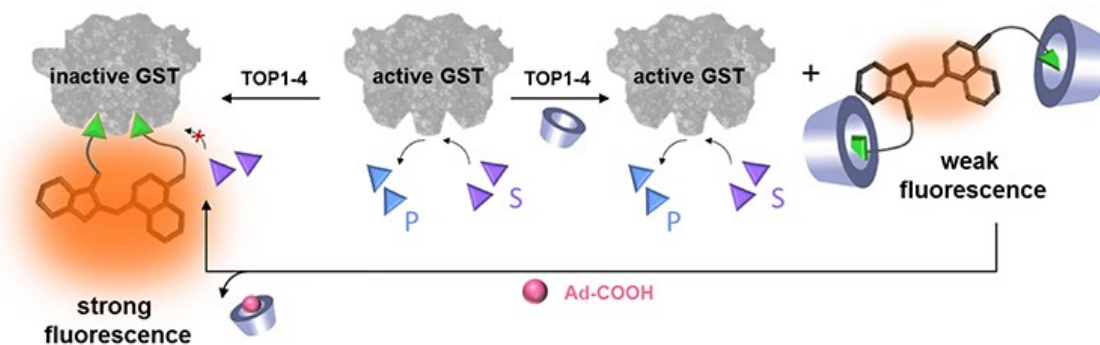
Figure 4: Logic gate TOPI-4 modulation of activity of GST dependent on chemical stimuli[33]

Sensitivity towards certain stimuli in molecular logic gates is given by functional groups capable of interaction with given compounds (resp. stimuli). By utilizing reactivity towards reactant or product of enzymatic reaction, enzyme-reactive logic gates, or logic gates sensible towards enzyme substrates/products can be constructed.

Great example of such mentioned system can be peroxide sensible gel with arylboronic acid functionalization mentioned before,[25] irreversibly reacting with hydrogen peroxide to produce compounds unable of self-assembly therefore causing liquification of gel. Utilizing glucose-oxidase enzyme producing peroxide in reaction to glucose, can lead to glucose sensitive system. In similar manner, other oxidases (choline-oxidase, sarcosine-oxidase) were used to produce gels reactive to different enzyme substrates. Combination of such enzymes in gels lead to gel reactive

towards multiple substrates, thus exhibiting OR gate behavior, with interesting selectivity given by enzymes (Figure 5).
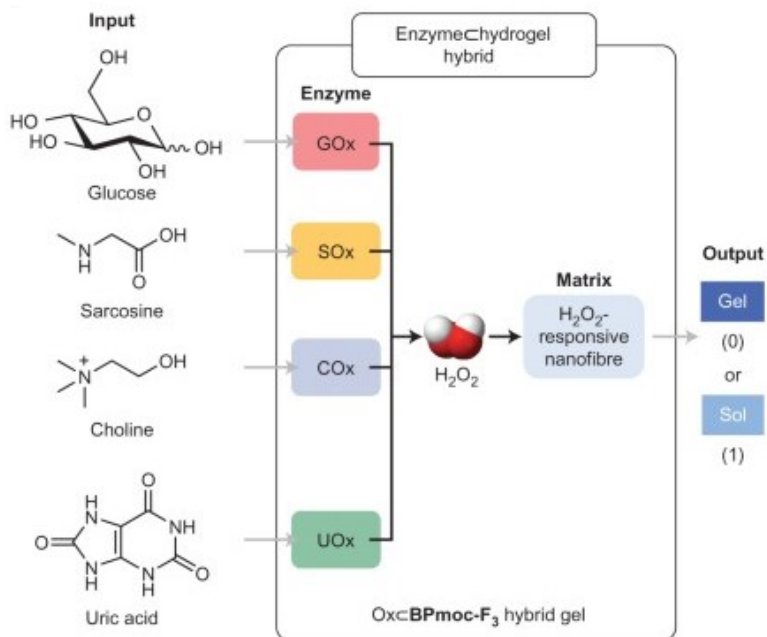
Figure 5: Enzyme-hydrogel hybrid capable of reactivity towards enzymes substrates[25]

Example worth mentioning of directing sensitivity via functional groups is gelator with naphthaldehyde aldimine group (Figure 6).[34] Phenolic OH group shows reactivity towards hydroxide anions and therefore changes in pH. Structural part identical with salicylaldimine, well known to form complexes with metal cations causes reactivity towards copper(II) cations, which in combination with reactivity towards bases mentioned before can be regarded as OR gate behavior.
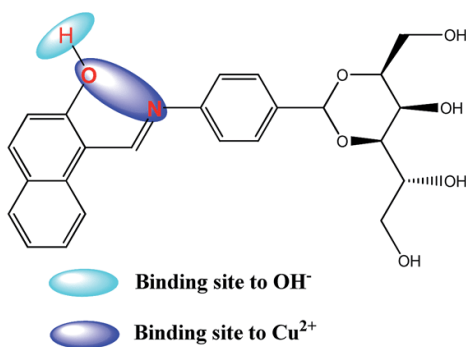
Figure 6: Naphthaldehyde-aldimine gelator[34]

2.4. Urease

Urease (urea amidohydrolase EC 3.5.1.5) is metalloenzyme belonging to group of hydrolases, catalyzing hydrolysis of urea to produce carbon dioxide and ammonia.

Urease was first enzyme that was recognized to be protein and that was isolated from beans in amount high enough to be crystallized by Prof. Sumner, which was later in 1946 awarded Nobel prize for showing that enzyme is in fact a protein and for crystallizing enzyme.[35]

Besides historical importance, urease is common enzyme occurring in many species of bacteria, molds and plants. Presence of urease in human has been proved to be caused by bacteria. Presence of urease respectively urease activity is used as an important taxonomical tool for identification of unknown bacteria, many of which can be pathogenic and therefore testing for presence of urease in bacterial colony is important step in diagnostics of some illnesses.[36] One of well known urease expressing human pathogen is bacteria *Helicobacter pyroli*, which can cause gastritis, peptic ulcers. It is known that action of urease produced by *Helicobacter pyroli* helps bacteria to survive in host organism and is also capable of damaging tight junctions in tissue (ammonia produced has cytotoxic effect on human body cells).

Many tests have been developed for analysis of urease presence. For direct testing of presence of urease, electrophoresis can be used. Indirect tests are based on production of ammonia which presence can be analyzed by i.e. Nessler reagent, ion-selective electrodes or phenol-hypochlorite reaction.[37] Fast clinical tests are often based on indication of raising pH caused by production of ammonia, common indicator being phenol red with $pK_a = 8.00$. For this purpose standard agar media with added urea and pH indicator are commonly used. After cultivation, color change of agar is interpreted as positive result for presence of urease.

2.5. Characterization techniques

2.5.1. Electron microscopy (EM)

Resolution of the classical optical microscope is physically limited by the Abbe diffraction limit which is given by wavelength of electromagnetic radiation. Wavelengths of visible light fall in the range from 400 to 700 nm; using shorter wavelengths is limited by problems with either absorption of the radiation (in the UV-range) or refractive indices very close to one (in the X-ray range) thus it is difficult or even impossible to find materials for construction of lenses. Therefore, when higher magnification is needed electron microscopy can be used. In the case of electrons, their wavelength is given by the de Broglie equation, meaning that wavelength is dependent on momentum and therefore kinetic energy of electrons. The electron source is based either on thermionic emission (tungsten or LaB_6 filaments heated to high enough temperature under high voltage to start emitting electrons) or field emission (so-called field emission guns which emit electrons by applied electrostatic force). Electrons are accelerated by high voltage and manipulated by so called "electron optics". Because electron is a charged particle, it can be manipulated using electromagnetic fields; therefore, in the place of classical glass lenses, fields are generated by coils which deflect the trajectory of the electron beam.[38]

The scanning electron microscope (SEM) detects electrons either backscattered from the sample surface or emitted from the sample surface by its interaction with incident electron beam (so-called secondary electrons), therefore providing us with view on the surface of sample. When analyzing non-conductive samples by SEM, the material is being charged by electrons from the electron beam which causes distortion of the scan. This is why non-conductive samples are often coated with thin film of highly conductive metal (i.e. platinum) by sputtering. This film can also protect the sample from heat damage caused by the energy of electron beam dissipating into the sample.

Transmission electron microscope (TEM) detects electrons transmitted through the sample. The sample must be thin or made into thin sections for electrons to be able to pass through (often <150 nm, but this value depends on character of sample). In contrast to SEM which is giving us information about the surface, TEM can provide us with information about internal morphology of sample, going up to aberration-corrected TEMs with sub-ångström resolution.

2.5.2. Small angle x-ray scattering and wide angle x-ray scattering

Small angle x-ray scattering (SAXS) and wide angle x-ray scattering (WAXS) are scattering techniques used for non-destructive analysis of nano-structured materials or systems. In typical SAXS or WAXS experiment, sample is irradiated by monochromatic and narrow x-ray beam, which is scattered by sample, according to Bragg equation (1).

$$n\lambda = 2d \cdot \sin(\theta) \tag{1}$$

Where n is diffraction order, λ is wavelength used, θ is scattering angle and d is interplanar d-spacing. In known distance behind sample lays detector, where we detect diffraction pattern. Because extremely small angles correspond to large objects (considering sizes above 1 μm) these angles are filtered by beam stopper positioned between detector and sample.[39] From this equation we can easily see basic difference between SAXS and WAXS. SAXS is typically defined as measurement of angles from 0.1 up to 5 degrees, WAXS is commonly measured up to 60 degrees. If we calculate corresponding distances, SAXS is useful for identification of structures in size range of 10 to 500 Å (SAXS can be even used for low-resolution analysis of protein shape), while WAXS from 1 to 10 Å. SAXS is therefore capable of giving us information about shape, distribution of size, spacing in partially ordered samples, and surface-to-volume ratio.[40] WAXS give us useful information about crystallinity of sample and crystallite size. Crystallite size can be calculated using the Scherrer equation.

2.5.3. Atomic force microscopy (AFM)

Atomic force microscopy is special type of high-resolution scanning probe microscopy useful for characterization of sample surface up to sub-nanometer resolution. Main difference between AFM and more "classical" microscopy techniques mentioned above is that AFM doesn't utilize interaction of electromagnetic waves with matter, but mechanical interaction of probe with solid sample. The tip of the probe is deflected (by mechanical or Van der Waals forces) by the sample and such motion is amplified to be detected. Amplification is often done by mirroring laser beam from probe. Small changes in angle of probe, create noticeable differences in reflected beam position detected in distance. Measured deflection of beam can be related to height of sample by which the probe tip was deflected. By raster scanning through surface of the sample and obtaining many point heights, it is possible to recreate an image.

Nowadays, AFM is commonly performed in so called "tapping mode". This means that the tip of the probe is constantly oscillated at its resonant frequency and amplitude of oscillation is used to control height of the tip above sample. Beside classical height imaging, detection of phase shift of oscillation frequency can be also detected and plotted in similar manner, called phase imaging. Such image reflects various interactions of surface with tip, such as stiffness or adhesive properties, and can give us information also about internal structure of sample.[41]

3. Materials and methods

3.1. Construction of logic gates

Chemicals: 3-isobutoxyphenylboronic acid (PBA), pinacol, hydroquinone, dopamine hydrochloride, adenosine 5′-triphosphate monosodium salt (ATP) were supplied by Sigma-Aldrich. Sodium hydroxide, sodium bicarbonate, hydrochloric acid (35% aqueous) and potassium iodide were supplied by Lach-Ner. Urease preparate used (Urease from *Canavalia ensiformis*, with specific activity approximately 8 U/mg according to supplier) was supplied by Sigma-Aldrich and stored at -16 °C.

Gel samples has been prepared by dissolving 55 mg of PBA in 20 ml of boiling water and pipetting 0.7 ml of solution with micropipette with plastic tip to every glass vial while still hot and letting them cool freely to room temperature, leading to gel with 10 µmol of PBA gelator per vial (vials used in experiments were 2 ml).

In testing of each logic gate 2 samples of gel have to be used. To each sample, one of the inputs (either I_1 or I_2) is added and after 5 minutes output (either liquid (logical 1) or gel (logical 0)) is read. Afterwards another input to the previous is added and after 5 minutes output is read again in the same manner. This is done to ensure that in the case of presence of both inputs the output is not dependent on order of additions. Inputs as solutions or solids are always carefully added to surface of gel and let dissolve and diffuse through gel, amounts are optimized to take no longer than 5 minutes to give output. Output is defined as solution equal to 1 and gel equal to 0. In cases of NOT, NOR, IMPLY and NAND gates, 50 µl (1 molar equivalent to gelator) of 0.2 M sodium hydroxide solution was added to each vial prior to further additions of any inputs, causing dissolution of gel. This is done because all of the four mentioned gates have to give positive output without addition of any input.

Specifications of chemical inputs used for each gate:

AND gate (first variation):

I_1: addition of 12 mg (10 eq.) of solid sodium bicarbonate
I_2: addition of 12 mg (14 eq.) of solid pinacol

AND gate (second variation):

I_1: addition of 12 mg (10 eq.) of solid sodium bicarbonate
I_2: addition of 6 mg (3 eq.) of solid dopamine hydrochloride

OR gate:
I_1: addition of 50 µl (1 eq.) of 0.2 M sodium hydroxide solution
I_2: simultaneous addition of 12 mg (10 eq.) of solid sodium bicarbonate and 12 mg (14 eq.) of solid pinacol

INHIBIT gate:
I_1: addition of 50 µl (1 eq.) of 0.2 M hydrochloric acid solution
I_2: addition of 50 µl (1 eq.) of 0.2 M sodium hydroxide solution

To all further gates applies prior addition of equimolar amount of sodium hydroxide:

IMPLY gate:
I_1: addition of 50 µl (1 eq.) of 0.2 M hydrochloric acid solution
I_2: addition of 50 µl (1 eq.) of 0.2 M sodium hydroxide solution

NOT gate:
I: addition of 50 µl (1 eq.) of 0.2 M hydrochloric acid solution

NOR gate:
I_1: addition of 50 µl (1 eq.) of 0.2 M hydrochloric acid solution
I_2: addition of 6 mg (1 eq.) of solid monosodium salt of ATP

NAND gate:
I_1: addition of 3,5 mg (3 eq.) of solid hydroquinone
I_2: addition of 70 µl (1.5 eq.) of 6% Lugol solution prepared by dissolving 0.5 g of iodine and 1 g potassium iodide in 8.5 ml of water

3.2. Urease reactive gel

4 mg of arylboronic acid and 8 mg of urea have been dissolved in 2 ml of boiling water in vial, same sample has been prepared without addition of urea. After letting cool freely to room temperature gel has formed. Addition of 10 mg of urease preparate causes urea doped gel to liquify in course of 30 minutes. Control run with gel without urea addition has been done, which remained stable.

3.3. Preparation of gel doped with urea for rheometry

Three samples of gel were prepared by dissolving 6 mg of PBA and given amount of urea (either 10, 20 or 30 mg) in 3 ml of boiling water and letting them cool freely to room temperature. Sample with 100 mg of urea per 3 ml of water has been prepared as well but haven't solidify even after cooling to 6 degrees in fridge overnight.

3.4. Attempts at crystallization of arylboronic acid

We have attempted to produce crystals of arylboronic acid for further XRD characterization. Slow solvent evaporation in vials covered with aluminum foil in course of few days has been tried. Solvents tried were acetonitrile, acetone, chloroform, hexane and dioxane. PBA has been found to be insoluble in hexane. None of samples produced crystals, product after evaporation looks either as amorphous mass or under light microscope there are visible fibers similar to that we observe in gel. Attempts at crystallization by slow cooling from water contained in Dewar flask always led to gel.

3.5. Capillary Microcalorimetry

Microcalorimetry measurements were performed with a *Nano DSC, TA Instruments-Waters LLC, New Castle, USA*. The microcalorimeter consists of sample and reference capillary cells of volume 0.3 mL (platinum). 3 samples of gel has been prepared by dissolving 2.04 , 2.70 , 3.54 mg of PBA per 1 ml of boiling water and letting them freely cool to room temperature. Before analysis, samples were preheated to liquify gel. The sample cell was filled by overfilling with ca. 0.6 mL of sample solution, reference cell has been filled with deionized water. In case of sample with 6 mg/ml of PBA the cell had to be preheated as well to 80 °C. The measurements were performed under constant pressure 3 atmospheres with temperature span from 5 to 80 °C. For each sample, series of two consecutive heating and cooling scans were performed to confirm reproducibility. After each sample, the cell has been cleaned by flushing with 2 liters of deionized

water. Reported data are subtracted of measurement of deionized water which was done the same day.

3.6. Small angle x-ray scattering (SAXS) and wide angle x-ray scattering (WAXS)

The SAXS experiments were performed using a pinhole camera (Molecular Metrology SAXS System) attached to a microfocused X-ray beam generator (*Osmic Micro-Max 002*) operating at 45 kV and 0.66 mA (30 W). The camera was equipped with a multiwire gas-filled detector with an active area diameter of 20 cm (Gabriel design). Two experimental setups were used to cover the q range of 0.04 - 11 nm^{-1}. Scattering vector $q = (4\pi n/\lambda)\cdot\sin(\theta)$, where $\lambda = 0.154$ nm is the wavelength and θ is the angle between the incident X-ray beam and the detector measuring the scattered intensity. Glassy carbon sample, obtained from Rigaku Company (Japan), was used to measure intensity.

Wide-angle X-ray scattering (WAXS) experiments were performed using a pinhole camera (Older Rigaku *SMAX2000* upgraded by SAXSLAB/Xenocs) attached to a microfocused X-ray beam generator (*Rigaku MicroMax 003*) operating at 50 kV and 0.6 mA (30 W). The camera was equipped with a vacuum version of a Pilatus 300K detector. The experimental setup covered a q range of 0.004-3 Å^{-1}. Scattering vector, q, is defined as: $q = (4\pi n/\lambda)\cdot\sin(\theta)$ where λ is the wavelength and θ is the scattering angle. Calibration of primary beam position and sample-to-detector distances was performed using the Si powder sample.

3.7. Scanning electron microscopy (SEM)

Morphology of the nanofibrous hydrogel structure was also confirmed by scanning electron microscopy (UHR SEM MAIA3, Tescan s.r.o). The drop of liquid sample was placed on the fresh mica surface and left to completely dry at room temperature. Prior to SEM examination, a conductive thin Pt film was deposited on samples surface by vacuum sputter coater: *SCD 050* (Balzers), *SCD 050* (Leica). The sample was examined in high vacuum mode at typical operating voltage 10 keV. Analysis of the pictures has been done in *ImageJ*.

3.8. Transmission electron microscopy (TEM)

Transmission electron microscopy micrographs were obtained using a JEOL NEOARM transmission electron microscope (JEOL, Japan) operating at an acceleration voltage of 200 kV and equipped with a TemCamXF416R 4k×4k CMOS camera (TVIPS, Germany). The homogenized solid sample of xerogel was deposited on a copper TEM grid coated with lacey amorphous carbon film. Analysis of the pictures has been done in *ImageJ*.

3.9. Rheometry

The rheological experiments have been done on a strain-controlled ARES-G2 rheometer (from TA Instruments, USA), using a parallel plate fixture with a diameter of 25 mm. Standard sample.

Strain sweep tests were carried out in order to find a range of deformation values, where the deformations do not damage the physical network in the studied gels. The tests were carried out as follows: The investigated monomer solutions were heated to 80°C and stirred at this temperature for 10 min. Subsequently, they were loaded between the parallel plates of the rheometer (which also had 80°C). Thereafter, the sample was left to cool down to room temperature and gelate (15 min waiting time). The oscillatory experiment mode was selected, with a constant frequency of 1Hz, while the deformation amplitude was set to be varied in the range from $2\cdot10^{-3}$ to 500 % (ascending values). The obtained rheological results were evaluated,

and the 'safe' value of the deformation amplitude was chosen as 1/10 of the deformation amplitude, below which the dynamic moduli (G', G'') started to be frequency-independent. The so-obtained 'safe' deformation amplitude (0.01%) was then used in the gelation tests.

The gelation process of the different PBA solutions was investigated as follows: The tested solutions were initially heated to 80°C (and stirred at this temperature for 10 min). Subsequently, they were put between parallel plates also pre-heated to 80°C. After sample loading, the rheology test was started, while the studied system was simultaneously cooling-down by contact with the ambient air. In this way, the rheological properties were recorded simultaneously with the directly measured (embedded contact thermometer) temperature of the plates. The time-dependent dynamic shear storage modulus $G'(t)$ and loss modulus $G''(t)$ were measured in oscillatory measurements at the frequency of 1 Hz and at the strain amplitude of 0.01% (which was previously determined in the strain-sweep-test, and found not to damage the physical crosslinks in the gel - 'linear deformation region'). The obtained values of the time-dependent sample temperature $T(t)$ made possible to depict the obtained rheology results as temperature-dependent moduli $G'(T)$ and $G''(T)$. The temperature of gelation was defined as the one of G' / G'' cross-over (G' is higher in the gel phase).

3.10. Atomic force microscopy (AFM)

The samples for atomic force microscopy characterization were prepared on freshly cleaved mica. Gel sample has been prepared by dissolving PBA in hot water (2 mg/mL) and letting freely cool to room temperature. The cleaved mica was dip coated in the gel sample and dried freely in the air in dust free conditions. Atomic force microscopy measurements were performed in the tapping mode under ambient conditions using an NT-MDT Ntegra Prima scanning probe microscope equipped with a *Nanosensors* silicon cantilever. The AFM measurements were using *NovaTM* software *NT-MDT Solver NOVA 1.1.0.1851*. Obtained images were fitted by average in one-dimensional flatten correction and subtracted by 3rd order polynomial surface in two-dimensional flatten correction. Fiber thickness has been measured in *ImageJ*.

4. Aims of thesis

In this thesis, we aim to describe new and simple LMW gelator, 3-isobutoxyfenylboronic acid, in the following steps:

1. Characterization of supramolecular and microscopic structure of PBA gel.
2. Tuning and characterization of thermal and mechanical properties of stimuli-responsive PBA gel.
3. The development of the logic gates for new phenylboronic acid (PBA) gel.

5. Results and discussion

5.1. Gel characterization by X-ray scattering (SAXS and WAXS)

From WAXS measurement (Figure 7) we can clearly see several reflections, the sample of hydrogel seems to be rather crystalline. Peak at $q = 0.60$ A^{-1} is matching d-spacing seen from TEM (Figure 9). After peak deconvolution procedure we can calculate degree of crystallinity as a ratio of crystalline peaks area to whole area. The calculation results in 52-53% (depending on whether we count the first high peak at $q = 0.36$ A^{-1} or not). Estimated size of crystalline domains is approximately 20 nm according to Scherrer equation. Because of crystallite size being much smaller than size of fibers we can assume that fiber is composed of small crystallites interacting together and glued by amorphous phase.
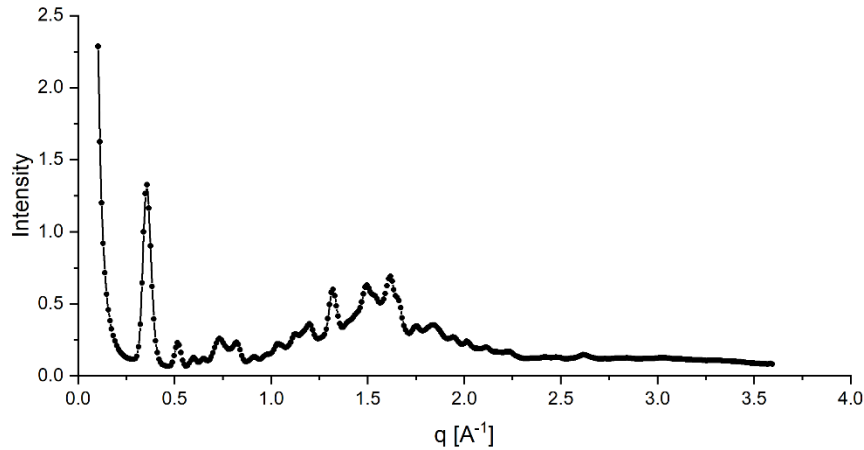
Figure 7: WAXS measurement of sample of PBA hydrogel

We have not observed any correlation peaks in the SAXS curve (Figure 8), therefore we cannot see any kind of organized structures within scale of 6 - 150 nm. From the regression of log-log plot we can clearly see that intensity through whole spectrum is directly proportional to q^{-4} which is in accordance with Porod's law, however particle surface cannot be determined from this measurement. The deviation at lower q values could be region which is intermediate between Guinier region and Porod region.

Regression	y = a + b*x
Intercept	-6.09498 ± 0.010
Slope	-3.99696 ± 0.008
R-square	0.9985
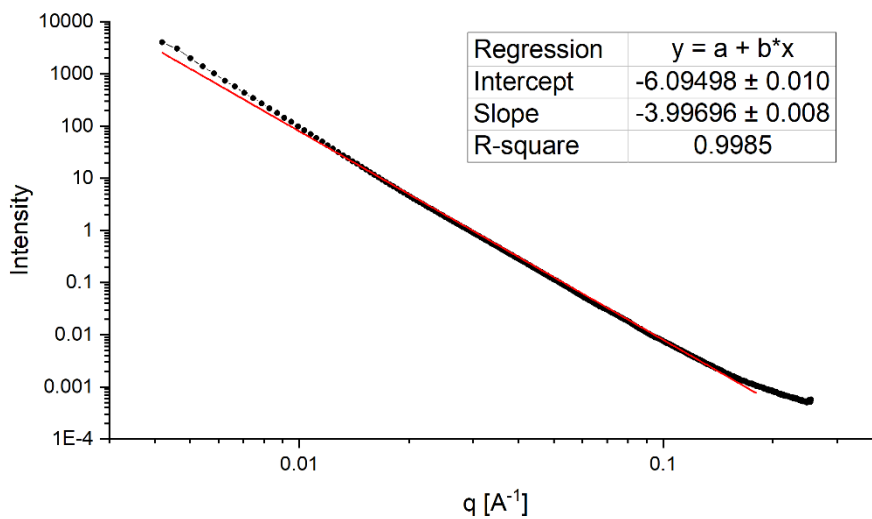
Figure 8: SAXS measurement of sample of PBA hydrogel

5.2. Gel characterization by transmission electron microscopy

In the HRTEM micrograph of the PBA xerogel sample we can distinguish both crystalline and amorphous phases. Analysis of the diffraction pattern obtained by FFT analysis of the micrograph is difficult as the image shows various spatial orientations of lamellar structures, however, periodical spacings of 1.1 nm (maxima 1 and 2) and 1.5 nm (maximum 3) can be clearly distinguished. Periodical spacing of 1.1 nm corresponds to visible lamellar structure of crystal. Presence of two maxima for the periodic spacing of 1.1 nm can be explained by different orientations of crystals in plane. It is noteworthy that the spacing of 1.1 nm is close to the d-spacing of 1.05 nm obtained from WAXS analysis. Suspected amorphous phase is missing any features in FFT analysis, confirming absence of ordering. (all presented pictures are adjusted in contrast for better visibility of structures, FFT has been also despeckled)
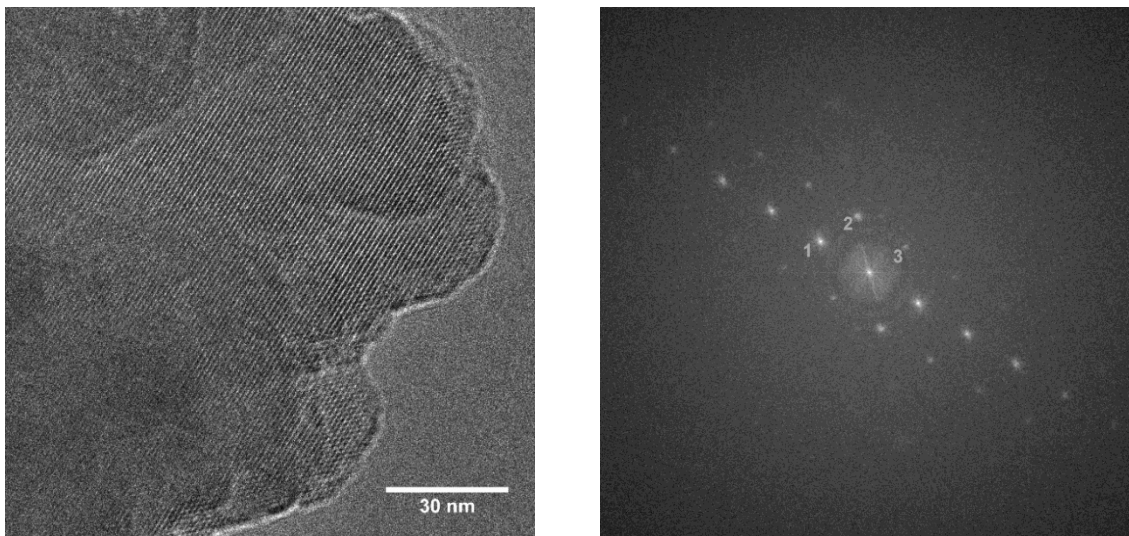
Figure 9: HRTEM image of crystalline phase of PBA xerogel (left) and its annotated FFT analysis (right)
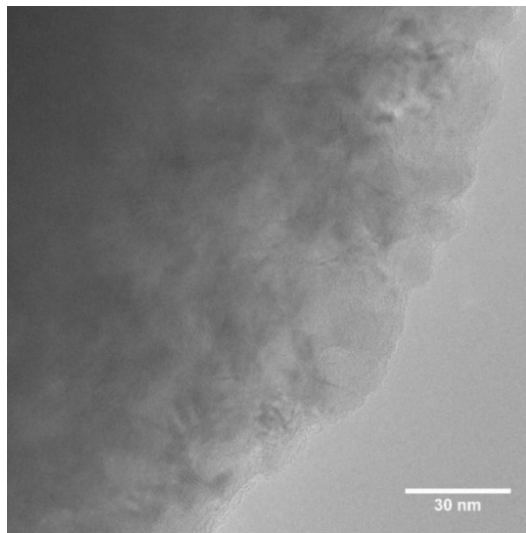
Figure 10: HRTEM image of suspected amorphous phase of PBA xerogel

5.3. Gel characterization by scanning electron microscopy

Fibrous character of hydrogel has been further confirmed by SEM. From Figure 11 and Figure 12 we can see that fibers are either very variable in thickness (thinnest fiber approximately 10 nm and thickest being 400 nm) and even thickness of single fiber is variable through its length, or the variability in thickness is caused by different spatial orientations of flat fibers. From Figure 12 we can also see branching of fibers (marked by yellow arrows) and absence of any preferable orientation.
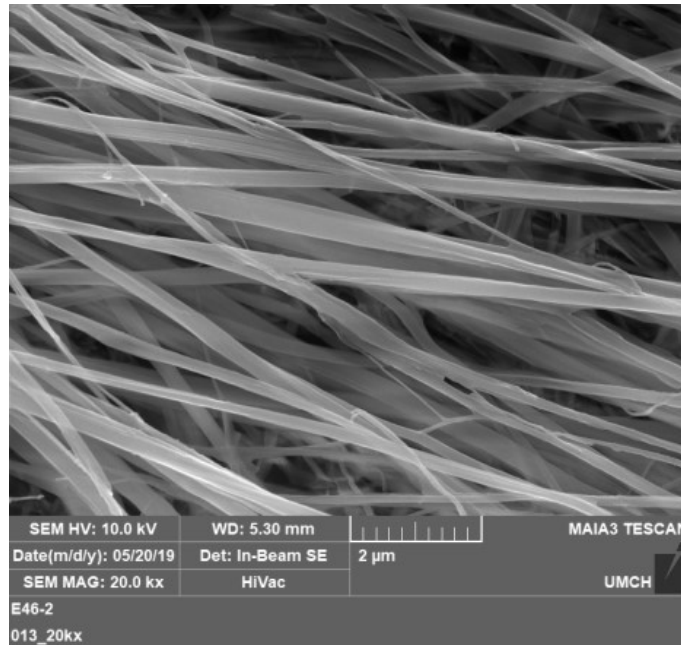
Figure 11: SEM image of sample of dried gel
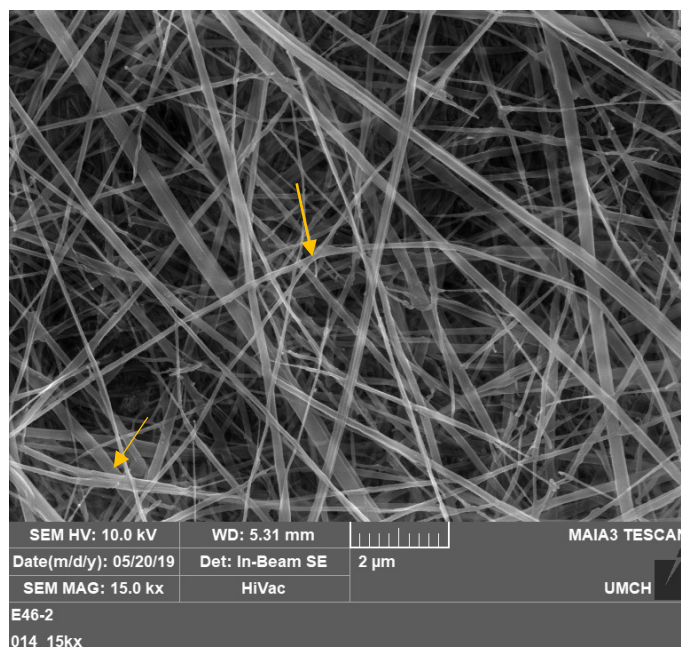
Figure 12: SEM image of sample of dried gel (branching marked by yellow arrow)

5.4. Gel characterization by atomic force microscopy

Atomic force microscopy of dried gel sample revealed similar structure to that seen from SEM. Fibers of thickness up to 2 microns can be seen (Figure 14). This can be due to the fact that dip coating itself can have effect on size selection of fibers and also because sample has been prepared by slow undisturbed cooling in vial. From Figure 13.A, fiber crosslinking and branching can be clearly seen. Phase contrast image (Figure 13.B) reveal fibrillar structure of single fiber. It is possible that in the process of gel formation newly formed fibers can act as nucleation site which lead to extremely variable fiber thickness, which can be seen on AFM as well as on SEM. Ribbed structure of edge of the fiber seen on phase contrast images is most possibly an artifact caused by oscillation of scanning probe as this effect can be seen only in horizontally oriented fibers. Imaging of PBA gel at higher magnification was not possible to obtain because of nature of the sample (fibers are very soft and easily dragged by the probe, mentioned distortion can be also seen in Figure 13.B, especially on bigger fibers). Interestingly from Figure 13.B we can clearly see that besides branching, intergrowth of fibers is present. This suggests that besides "standard" crystallographic mismatch branching[42] either intergrowth, or crystal twinning occurs.
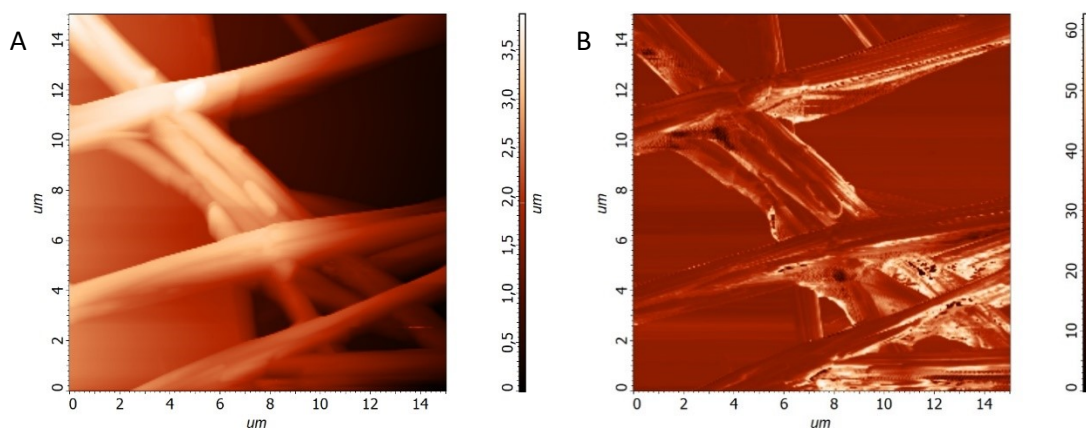
Figure 13: AFM images of sample of dried gel A - height and B - phase
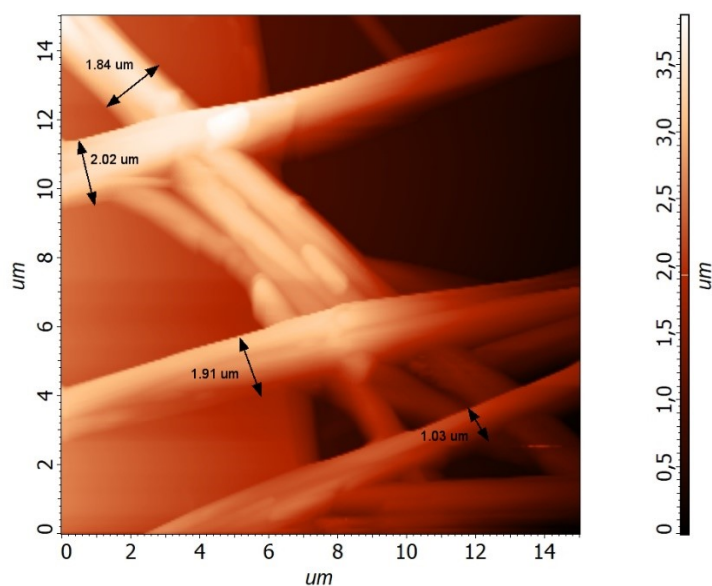
Figure 14: AFM height image of PBA dried gel with measured fiber-thickness

5.5. Capillary microcalorimetry:
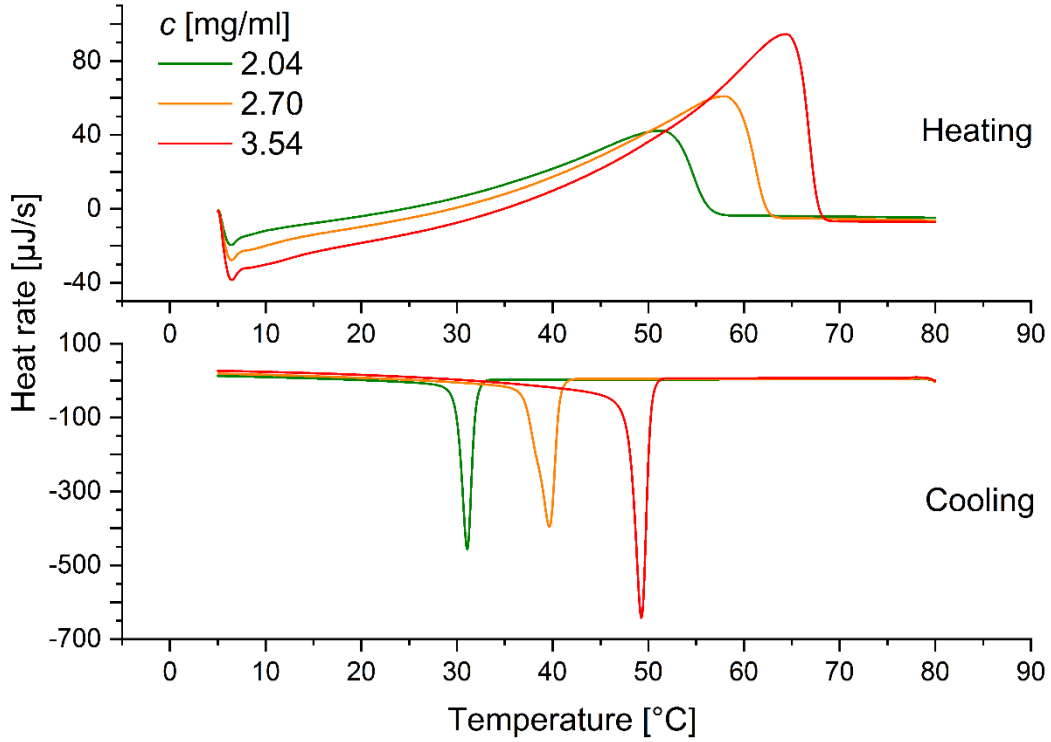
Figure 15: Capillary microcalorimetry of PBA hydrogel at different concentrations of PBA

The DSC cooling curves (Figure 15) show that the gelation temperature in the undisturbed sample is highly dependent on the gelator concentration (31.4, 39.8 and 49.4 °C for 2.04, 2.70 and 3.54 mg/ml of PBA respectively). This is no surprise and has been described many times for LMW gelators, with actually only a few explanations as to why. Ferry et al.[43] derived an equation for the variation of gel-sol transition temperature as function of concentrations of gelator and crosslinks, which after ignoring the enthalpy of crosslinking is applicable for LMW gelators.[44] This can be further explained by using the Van't Hoff equation (2), where we focus on the gel dissolution equilibrium described by the equilibrium constant $K = a_{ds}/a_s$ where activities of solid a_s and dissolved gelator a_{ds}. From scanning electron microscopy (Figure 11 and Figure 12) it is visible that gel formation is accompanied by gelator separation from aqueous phase into its own phase, creating network of gel. Concurrently, the WAXS measurement demonstrate that the gelator is even somewhat crystalline. Therefore, we can assume its activity equal to one for solid gelator ($a_s = 1$). In moment just before sol to gel transition, we can relate activity of dissolved gelator to its concentration. T can be though of as sol to gel phase transition temperature, H_t is transition enthalpy and R is gas constant.

$$\ln\left(\frac{K_1}{K_2}\right) = \ln\left(\frac{\frac{a_{ds2}}{a_s}}{\frac{a_{ds1}}{a_s}}\right) = \ln\left(\frac{a_{ds2}}{a_{ds1}}\right) = \frac{H_t}{R}\left(\frac{1}{T_2} - \frac{1}{T_1}\right) \tag{2}$$

In the case of heating curves (Figure 15), a similar dependence of gelation temperature on concentration can be seen. However, both the difference between gelation temperature of the heating curves compared to that of cooling curves as well as long tailing of the heating curves are apparent. Therefore, we theorize that this can be caused by solubility-limited dissolution of gelator. The tailing region matches for all concentrations most probably because at lower

concentrations the amount of gelator that can be dissolved (and therefore the absorbed heat) is limited by its solubility at the given temperature. A very similar difference between shape of heating and cooling curves in DSC experiments has been seen with compounds forming supersaturated solutions[45] and undercooled melts.[46] It has been suggested that gels prepared by cooling of solution are first in state of supersaturated solution which at some moment spontaneously either crystallizes, precipitate as amorphous mass or combination of both, which yields a gel.[24] We therefore suggest that PBA gelator easily forms supersaturated solution which while cooling at some critical point precipitates as combination of amorphous and crystalline phase in such manner that aggregation is favored in one dimension. This wouldn't cause any problems for the dependence of gelation temperature on concentration in cooling experiments, as the same equation holds true, and has been used for the description of crystallization of supersaturated solutions.[47]

5.6. Viscoelastic properties of hydrogel
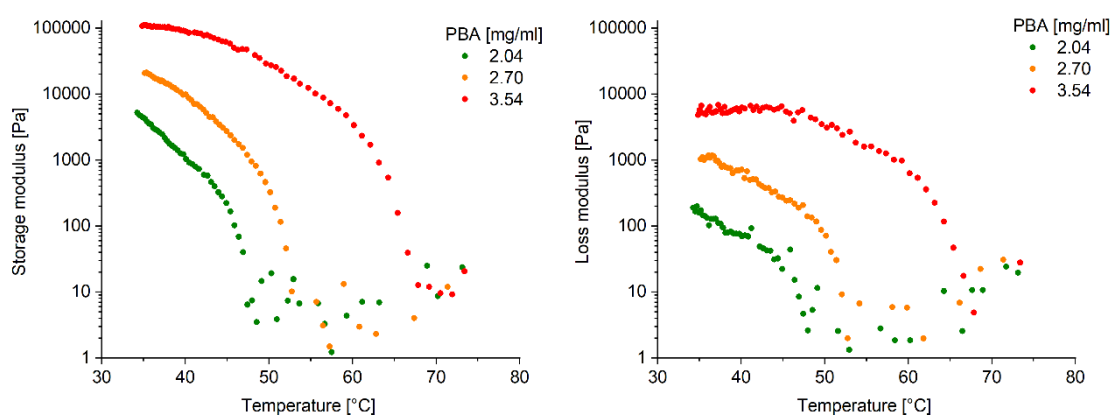
Figure 16: Temperature dependence (cooling experiment) of loss and storage modulus of PBA hydrogel at different concentrations of PBA

From rheology data (Figure 16) we can see, that with increasing concentration of PBA gelator, there is an increase in both storage and loss modulus (the chaotic region of lower temperatures in graphs is caused by artifact of measurement moduli under measurement limits in solution phase, these parts of plots are of no interest). Concerning the storage modulus (G'), higher concentrations of PBA expectedly lead to a denser gelator network. Interestingly, it was found by TEM (Figure 9) that the PBA network is not a simple hydrogen-bridged network made of individual PBA molecules. This network is in fact made of fiber-like microcrystallites combined with amorphous solid phase of PBA (Figure 10), which act like elastic chains in a classical elastomer network. Hence, a higher PBA concentration yields a stiffer elastic gel (macroscopic network of crystallites), so that we observe a higher storage modulus (G'). Also the increasing loss modulus (G'') can be explained in a similar way: At higher concentration and therefore denser gelator network, there also occurs more internal friction in and between the microcrystalline fibers from which the macroscopic gelator network is made. This friction leads to a higher loss modulus (G'').

Note: The most sensitive way to determine gelation point would be to perform a multi-frequency experiment, and to find the point at which the loss factor is frequency-independent. This point (according to the Chambon-Winter theory) is the point of gelation (time or temperature resp.). A limitation of the multi-frequency experiment is, however, that gelation must be sufficiently slow in comparison to the slowest frequency of the test, which is not the case of our gel. So, in our situation, the gelation temperature, in case of rheology, was defined as the crossover point of storage and loss modulus. This method of gel point definition is frequently used for abrupt

gelation processes, but the position of the gel point is frequency-dependent. Additionally, a source of inaccuracy might be due to the fragility of the PBA network. Oscillatory deformation (the rheological test itself) can lead to a delayed gelation, because of mechanical damage to the forming network.[48] Precaution was taken by choosing a small (0.01%) strain amplitude for all gelation tests.

When comparing data for gelation temperature from DSC cooling experiments and from rheology (gelation temperatures in case of rheology are 48.5 and 53.4 °C for 2.04 and 2.70 mg/ml PBA respectively, in case of 3.54 mg/ml sample this could not be determined because of chaotic region interfering with crossover point), there is noticeable difference. In case of the DSC experiment, the studied sample is undisturbed and therefore able to stay in the state of supersaturated solution, while in the rheology experiment, the sample is disturbed by the mechanical oscillations, which can trigger crystallization and thus prevent the before mentioned supersaturation (and undercooling). For these reasons, the gelation temperatures from rheology are closer to the gel to sol transition temperature from DSC heating curves. Additionally, in case of the DSC heating curve directly detects the heat of melting, but not directly the mechanical reversal of gelation, which might be shifted. Also, it is noteworthy that the rates of temperature change were somewhat different in DSC and rheology, although this should not lead to such noticeable difference.

5.7. Urea effect on gel viscoelastic properties

While studying urease reactive gel we noticed that addition of urea causes changes in gel transition temperature and mechanical properties of gel. When preparing sample with concentration of approximately 33,3 mg/ml of urea, gel haven't form even after cooling overnight in fridge down to 6 °C. We further studied impact of lower concentrations of urea on formation of gel going up to 10 mg/ml.
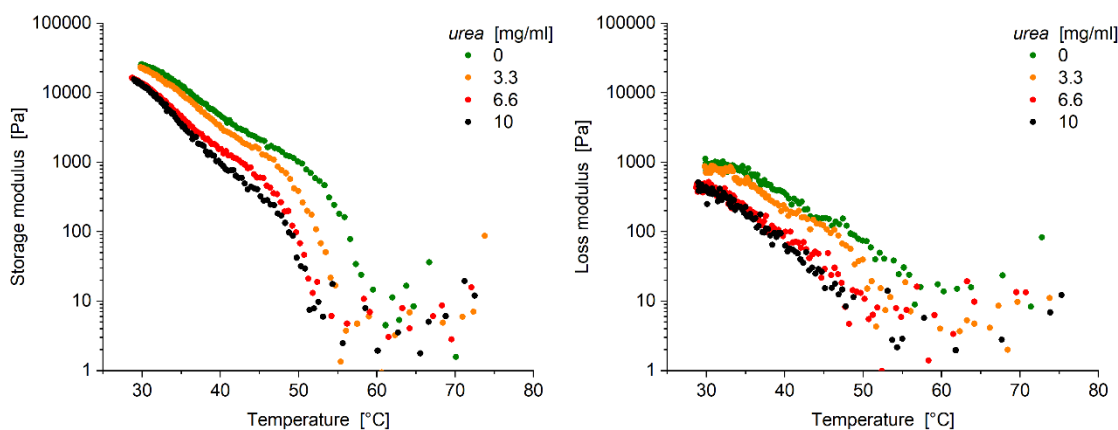
Figure 17: Temperature dependence (cooling experiment) of loss and storage modulus of urea doped PBA hydrogel

In Figure 17 we can see temperature dependence of storage and loss modulus of PBA gel at same concentration of gelator, doped with either with 0, 3.3, 6.6 or 10 milligrams of urea per milliliter of gel with same concentration of PBA gelator (again the chaotic region of lower temperatures in graphs is caused by artifact of measurement moduli under measurement limits in solution phase, these parts of plots are of no interest).

As stated before in case of PBA gel gelation temperatures has been determined from rheology as crossover point of storage and loss modulus. Gelation temperatures determined in this way are 57.3, 54.1, 51.3 and 50.8 °C for 0, 3.3, 6.6, 10 mg/ml of urea respectively. Clear trend of

decreasing of gelation temperature with increasing concentration of urea can be seen. This possibility of tuning melting temperature could be used in refrigerated transport for indication of that temperature never raised above threshold. Gel with metal ball on top contained in sealed ampoule would in case of overheating melt, and ball would fall to the bottom of ampoule, indicating problem (similarly to folk trick with coin on top of ice in fridge, indicating that fridge wasn't working for some time if coin is found under ice).

Change in physical properties and melting temperature could be caused either by chaotropic behavior of urea capable of disrupting hydrogen bonding, or lone electron pairs on nitrogens capable of interacting with boron on PBA via donor-acceptor bonding. Further experimental research is needed to confirm either of assumptions. Chaotropic effect could be verified by using other chaotropic agent without ability of forming donor-acceptor bonding with boronic acids, for example lithium acetate or even better lithium perchlorate. In case of confirmation of chaotropic effect, addition of non-basic kosmotropic agents like ammonium or lithium sulphate should be studied for antichaotropic (kosmotropic) effect, and even better tuning of gel physical properties.

This possibility of tuning of viscoelastic properties, by external chemical stimuli, of hydrogel could be extremely interesting for tissue scaffolding and altering of differentiation of stem cells. Urea is relatively non-toxic to human cells and in case of our PBA gelator capable of large changes in elastic properties, similar to changes done by altering of alkyl chain-length.[27] More research has to be done to prove this concept such as studies of biocompatibility of PBA, but if these conditions are met, system of only PBA and non-toxic urea would be enough to offer large spectrum of different elastic properties.

5.8. Logic gates

Logic gates using PBA can be made by utilizing reactivity of arylboronic acids with 1,2-diols to form cyclic esters and acidic properties of boronic acid and its esters. Esters of simple arylboronic acids are in general more acidic. In all experiments gel state corresponds to 0 and solution to 1.

Difference in acidity of simple PBA and its ester was used to prepare AND gate. Because pK_a of free acid is approximately 8.5,[49] the gel is unreactive towards addition of bicarbonate, and gel itself is not reactive with pinacol at noticeable rate, only addition of both can shift equilibrium towards soluble salt of esterified PBA (Scheme 4), and therefore dissolve gel. Dissolution of gel is quite slow so excess of both reagents needs to be used. High excess of any of two reagents doesn't cause any problems.
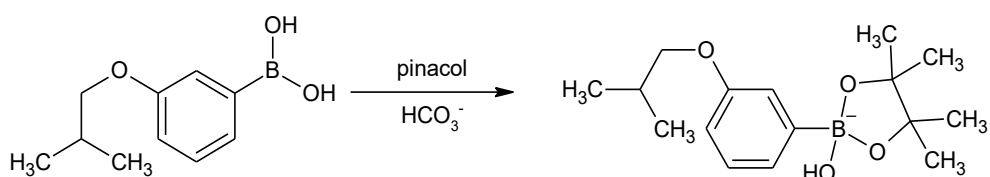
Scheme 4: Reaction leading to tetrahedral phenylboronate salt
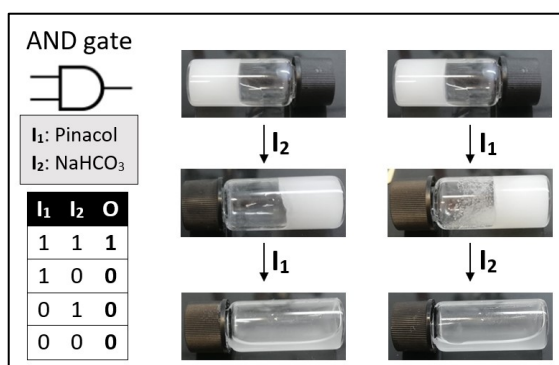
Figure 18: PBA based AND gate

This mechanism can be used for catechols as well, in our particular example exchanging pinacol with dopamine hydrochloride (Scheme 5) leads to effective AND gate as well.
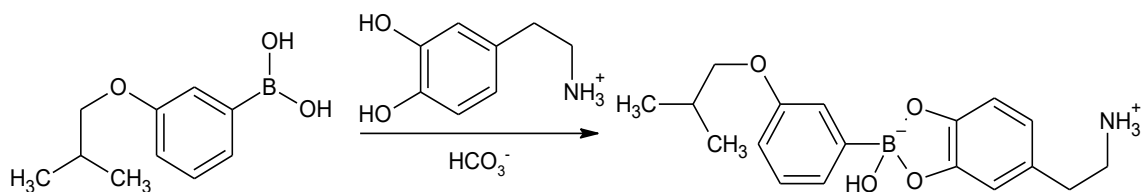
Scheme 5: Reaction leading to tetrahedral dopamine ester of phenylboronate salt

OR gate has been made by combining positive output of AND gate as one input and neutralization reaction of arylboronic acid with sodium hydroxide as the second. First input corresponds to addition of strong base, in this case sodium hydroxide, to produce salt (Scheme 6) and second input corresponds to addition of solution of sodium bicarbonate and pinacol. This also shows how two gates could be combined in simple manner to produce simple logic circuit.
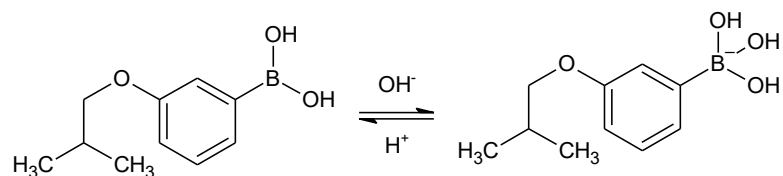
Scheme 6: Acidobasic reaction of phenylboronic acid
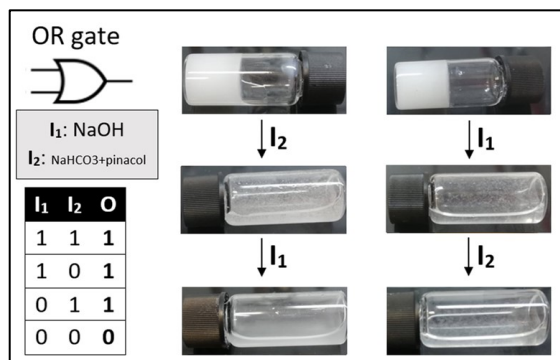
Figure 19: PBA based OR gate

In all gates where absence of both inputs lead to output 1, equimolar amount of sodium hydroxide solution has been added to gel prior to experiment to produce solution of phenylboronate (Scheme 6). NOT gate was afterwards produced by addition of equimolar amount of acid, causing neutral *phenylboronic acid* to form gel (output equals 0). This method has been used previously in gel containing arylboronic acid functionalization.[50] Amount of acid used has to be equimolar or in excess compared to sodium hydroxide used to dissolve gel.

NOR gate has been prepared in similar fashion as NOT gate, with one of the input being addition of strong acid, and second more interesting, addition of sodium salt of ATP, which undergoes hydrolysis to ADP and phosphate, neutralizing solution and producing gel (Scheme 7). It should be noted that further hydrolysis slowly occurs up to adenosine, therefore ATP isn't good candidate for production of comparator gates.
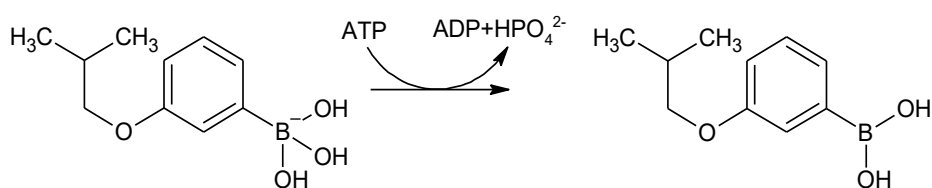
Scheme 7: ATP-hydrolysis driven neutralization
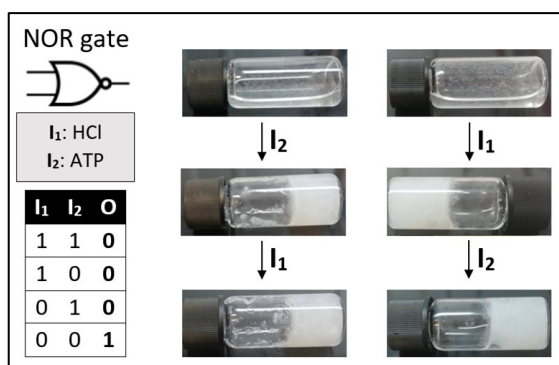
Figure 20: PBA based NOR gate

Furthermore, comparator gate can also be based on comparing amount of sodium hydroxide as one signal and hydrochloric acid as the compared signal. When sodium hydroxide is at least in equimolar (with gel) excess compared to hydrochloric acid added output correspond to 1, otherwise 0. Other possibility is, when using gel with equimolar amount of base added, by defining one input as equimolar addition of base and second as equimolar addition of acid simple version of IMPLY gate can be made. In the same manner, using gel without any added sodium hydroxide and again defining one input as equimolar addition of base, and second as equimolar addition of acid, INHIBIT gate (behaving as pH dependent on/off switch) can be made in similar way as in previously studied pH sensitive systems.[34]

Simple method to create NAND switch has been found by implementing redox reaction of hydroquinone and iodine which is able to cause sol to gel transition. Hydroquinone is even weaker acid than boronic acids, therefore it is not able to cause gelation on its own, and disproportionation of iodine under weakly basic conditions is quite slow. Redox reaction of hydroquinone with iodine, produces strong hydroiodic acid (Scheme 8). Hydroiodic acid is stronger acid than PBA, so only addition of both reactants can cause sol-gel transition. Solution of iodine and salt of PBA degrade with time (we suspect this to be caused by electrophilic substitution with iodine), depending on pH of starting solution, so reaction should be done in course of an hour.
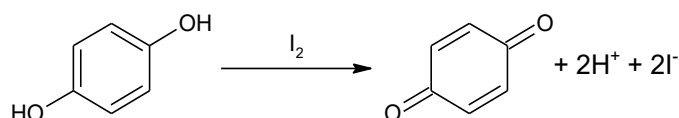
Scheme 8: Hydroquinone reaction with iodine
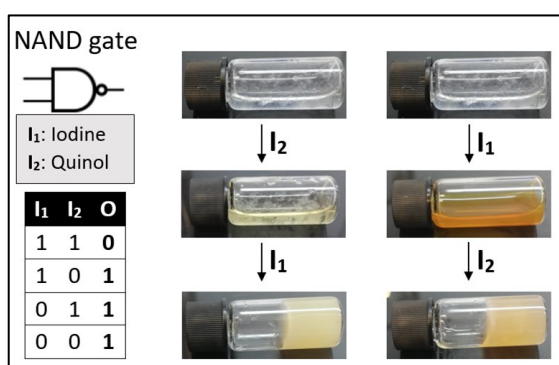
Figure 21: PBA based NAND gate

AND and NAND gates could have huge implications in drug delivery. As an example, releasing cytostatic drugs only in those parts of tissue with low pH and low oxygen levels at same time, which is characteristic for cancerous cells,[51] could help overcome otherwise unpleasant symptoms caused by nontargeted treatment (e.g. hair loss). As mentioned before arylboronic acids have highly tunable acidity of boronic group, some even up to physiological pH and reactions with 1,2-diols are of great interest because of their applications in glucose and fructose sensing. Combining these two properties with tuning of molecular response could be useful in selective insulin release as has been mentioned in state of art.[18] We have shown reactivity of gel towards dopamine, important hormone and neurotransmitter in most animals, and ATP, molecule responsible for energy transfer in almost all known living organisms (this reactivity is however not useable in biological systems as the reaction is based on pH change caused by ATP hydrolysis). To put sensitivity of such hydrogel in perspective, the amount of PBA needed for gelation is so small, that 1 cm^3 NOT gate can be triggered even by formic acid from single ant (calculation based on amount of acid in single ant[52]).

Because of simplicity of PBA gelator, all logic gates mentioned are based on reactions of phenylboronic acid, therefore it should be possible to apply most of logic gates on other systems with phenylboronic acid with similar pK_a. We constructed simple NOT and INHIBIT gates using similar acidobasic reactions as in previously studied pH responsive gelator,[34] we also show that IMPLY gate is easily accessible in similar manner to INHIBIT gate by changing starting pH. We further explored and simplified AND gate, based on complex equilibrium of PBA with pinacol ester dependent on pH and utilized this mechanism for dopamine, important hormone, and common target of molecular recognition with phenylboronic acids.[21,53] Other arylboronic acid based AND gates,[54] often utilize addition of weakly alkaline buffer as one of the inputs, because stronger bases would react with arylboronic acid without need for diol. In our case because of acidity not lowered too much by isobutoxy substitution, we were able to use sodium bicarbonate as pH modulating input instead of buffer. Because bicarbonate is only slightly alkaline, it cannot cause dissolution of gel without presence of diol. We further explored possibility of NAND gate preparation via pH change driven by redox reaction of hydroquinone and elemental iodine. There are many known redox reactions that are capable of producing pH changes in systems so this example can be further utilized for AND or NAND gates in other pH sensitive systems. However, caution must be taken that many organic compounds including phenylboronic acids are highly sensitive towards strong oxidation reagents, which could lead to irreversible degradation. OR and NOR gates were prepared based on multi-stimuli responsiveness of arylboronic acid. There are still many more interesting systems yet to be studied. Interesting photoreactive system has been made by photoacid triggered aggregation of similar LMW gelator.[55] Sensitive tuning and doping of PBA gel by such photoacid could provide gel with sensitivity towards another stimuli. Even more interesting results can be obtained by using reversible photoacid.[56]

5.9. Urease sensitive gel

Urease sensitive gel has been prepared by addition of urea when preparing gel. As we know from previous experiments, gel is pH sensitive, when pH is raised, gelator is dissolved as tetrahedral anion. Urea is practically stable towards hydrolysis in aqueous solutions, urease catalyzes hydrolysis of urea to carbon dioxide and ammonia (Scheme 9) and as result of this hydrolysis pH of solution is raised, causing dissolution of gel.
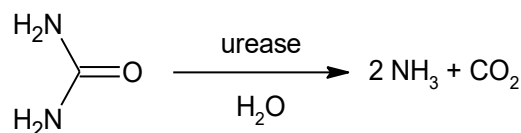
Scheme 9: Urease catalyzed hydrolysis of urea

Action of urease has been checked on gel without added urea, (the gel could be dissolved if urease sample contained anything basic, without need for catalytic action), and it was proved that reaction was indeed caused by catalyzed hydrolysis of urea. Tests for presence of urease are commonly used in identification of unknown bacteria, expression of urease by bacteria is one of important characteristics still being used. Even in standard rapid diagnostic tests for *Helicobacter pylori* (bacteria causing gastritis and stomach ulcers), urease tests are being used as rapid and good indicator for analysis of bioptic samples.[57] Indication by gel-sol transition could be more effective and visible than standard phenol red indicator for highly colored samples, although preparation of cultivation media based on PBA gel could be problematic.

Furthermore, it should be possible to easily implement this reaction in context of previously described logic gates. Urea-free gel itself is behaving as molecular AND gate where one of the inputs is urea and the second is urease. Only presence of both inputs can lead to liquefication of gel and therefore positive output, similarly to previously studied logic gates utilizing pH-indicator and urease catalyzed pH change.[58] Other logic gates can be possibly constructed utilizing this reaction but care must be taken because urease as well as other metalloenzymes can be sensitive towards high ionic strength, temperature and presence of strong chelating agents. Again, sensitivity of urease towards in example chelating agents could be regarded as INHIBIT gate behavior.

6. Summary and conclusion

We have discovered new LMW gelator of water, 3-isobutoxyphenylboronic acid (PBA), and characterized its physical and chemical properties. We characterized thermodynamic and viscoelastic properties of its hydrogels by means of capillary microcalorimetry and rheology. We attempted analysis of molecular structure of the gel by x-ray diffraction methods and analysis of gel microstructure by electron microscopy and atomic force microscopy.

PBA gelator has shown to easily form supersaturated solutions which after cooling, rapidly forms fibrous network of gel. Fibers are composed of mixture of amorphous and crystalline phase of PBA gelator (52% of crystalline material determined by WAXS). Similarly, to other gels, the PBA hydrogel is composed of network of solid gelator physically supporting water. Network of gelator is composed of fibers of extremely variable thickness (10-400 nm) which are branching and intersecting through whole volume of gel.

We have found that urea (non-toxic and biochemically important compound) has prominent effect on gel viscoelastic properties and its gelation temperature and examined this effect. Addition of urea to gel decreases both storage and loss modulus and lowers gelation temperature. This offers tuning of gel elastic properties by addition of non-toxic urea which can be useful for tissue scaffolding.

We studied reactivity of PBA hydrogel towards chemical stimuli, combinations of various chemical stimuli and interpreted these results in terms of logic gates. We prepared molecular OR, AND, IMPLY, INHIBIT, NOR and NAND gates with sol-gel response, and expanded AND and NOR gates function on dopamine and ATP inputs. We have also shown that OR and AND gate can be combined into simple logic circuit. We utilized acidity of PBA to produce AND gate based on pH (sodium bicarbonate) and diol (pinacol) inputs, without need of buffer. We have also shown how pH-modulating redox system can be utilized in the case of NAND gate. Furthermore, we prepared gel sensitive towards urease, enzyme commonly produced by many strains of pathogenic bacteria.

More research will be done to determine molecular structure of gel, such as solid-state NMR experiments. We want to further study biocompatibility of PBA gel and if possible, experiment with tissue scaffolding where stem cell differentiation is affected by changes in gels mechanical properties caused by external chemical stimuli.

7. Acknowledgment

8. References

1. Naahidi, S. *et al.* Biocompatibility of hydrogel-based scaffolds for tissue engineering applications. *Biotechnol. Adv.* **35**, 530-544 (2017).

2. Drury, J. L. & Mooney, D. J. Hydrogels for tissue engineering: scaffold design variables and applications. *Biomaterials* **24**, 4337-4351 (2003).

3. Li, J. & Mooney, D. J. Designing hydrogels for controlled drug delivery. *Nat. Rev. Mater.* **1**, 16071 (2016).

4. Hanabusa, K. & Suzuki, M. Development of low-molecular-weight gelators and polymer-based gelators. *Polym. J.* **46**, 776-782 (2014).

5. Ilic-Stojanovic, S. *et al.* Stimuli-sensitive hydrogels for pharmaceutical and medical applications. *Facta Univ. - Ser. Physics, Chem. Technol.* **9**, 37-56 (2011).

6. Lacina, K., Skládal, P. & James, T. D. Boronic acids for sensing and other applications - a mini-review of papers published in 2013. *Chem. Cent. J.* **8**, 60 (2014).

7. Ďorďovič, V., Vojtová, J., Jana, S. & Uchman, M. Charge reversal and swelling in saccharide binding polyzwitterionic phenylboronic acid-modified poly(4-vinylpyridine) nanoparticles. *Polym. Chem.* **10**, 5522-5533 (2019).

8. Marková, P. & Uchman, M. Synthesis and self-assembly of polyzwitterionic phenylboronic acid-containing double hydrophilic block copolymers. *Eur. Polym. J.* **151**, 110439 (2021).

9. Vrbata, D., Kereiche, S., Kalíková, K. & Uchman, M. Stimuli-responsive multifunctional micelles of ABC vs. ACB triblock terpolymers using reversible covalent bonding of phenylboronic acid: controlled synthesis, self-assembly and model drug release. *J. Mol. Liq.* **335**, 116528 (2021).

10. Matuszewska, A. *et al.* Glucose-Responsive Hybrid Nanoassemblies in Aqueous Solutions: Ordered Phenylboronic Acid within Intermixed Poly(4-hydroxystyrene)- block -poly(ethylene oxide) Block Copolymer. *Biomacromolecules* **16**, 3731-3739 (2015).

11. Ishiyama, T., Murata, M. & Miyaura, N. Palladium(0)-Catalyzed Cross-Coupling Reaction of Alkoxydiboron with Haloarenes: A Direct Procedure for Arylboronic Esters. *J. Org. Chem.* **60**, 7508-7510 (1995).

12. Hooshmand, S. E., Heidari, B., Sedghi, R. & Varma, R. S. Recent advances in the Suzuki-Miyaura cross-coupling reaction using efficient catalysts in eco-friendly media. *Green Chem.* **21**, 381-405 (2019).

13. Yuan, T., Xie, S. & Qian, C. Boron neutron capture therapy of cancer: Critical issues and future prospects. *Thorac. Cancer* **10**, 2195-2199 (2019).

14. Martínez-Aguirre, M. A., Villamil-Ramos, R., Guerrero-Alvarez, J. A. & Yatsimirsky, A. K. Substituent Effects and pH Profiles for Stability Constants of Arylboronic Acid Diol Esters. *J. Org. Chem.* **78**, 4674-4684 (2013).

15. Brooks, W. L. A., Deng, C. C. & Sumerlin, B. S. Structure-Reactivity Relationships in Boronic Acid-Diol Complexation. *ACS Omega* **3**, 17863-17870 (2018).

16. Lohse, M. S. & Bein, T. Covalent Organic Frameworks: Structures, Synthesis, and Applications. *Adv. Funct. Mater.* **28**, 1705553 (2018).

17. Huang, Q., Wang, L., Yu, H. & Ur-Rahman, K. Advances in phenylboronic acid-based closed-loop smart drug delivery system for diabetic therapy. *J. Control. Release* **305**, 50-64 (2019).

18. Zhao, F. *et al.* An injectable particle-hydrogel hybrid system for glucose-regulatory insulin delivery. *Acta Biomater.* **64**, 334-345 (2017).

19. Marinaro, W. A., Prankerd, R., Kinnari, K. & Stella, V. J. Interaction of Model Aryl- and Alkyl-Boronic Acids and 1,2-Diols in Aqueous Solution. *J. Pharm. Sci.* **104**, 1399-1408 (2015).

20. Wu, X. *et al.* Direct sensing of fluoride in aqueous solutions using a boronic acid based sensor. *Chem. Commun.* **50**, 13987-13989 (2014).

21. Hiller, N. de J. *et al.* Arylboronic Acids and their Myriad of Applications Beyond Organic Synthesis. *European J. Org. Chem.* **2020**, 4841-4877 (2020).

22. Caló, E. & Khutoryanskiy, V. V. Biomedical applications of hydrogels: A review of patents and commercial products. *Eur. Polym. J.* **65**, 252-267 (2015).

23. Skilling, K. J. *et al.* Insights into low molecular mass organic gelators: a focus on drug delivery and tissue engineering applications. *Soft Matter* **10**, 237-256 (2014).

24. Sangeetha, N. M. & Maitra, U. Supramolecular gels: Functions and uses. *Chem. Soc. Rev.* **34**, 821 (2005).

25. Ikeda, M. *et al.* Installing logic-gate responses to a variety of biological substances in supramolecular hydrogel-enzyme hybrids. *Nat. Chem.* **6**, 511-518 (2014).

26. Kanekiyo, Y. & Shinkai, S. CHAPTER 1. Supramolecular Chemistry of Boronic Acids. in 1-43.

27. He, J., Hu, Y., Wu, F., He, B. & Gao, W. Control of MSC Differentiation by Tuning the Alkyl Chain Length of Phenylboroinc Acid Based Low-molecular-weight Gelators. *J. Bionic Eng.* **15**, 682-692 (2018).

28. *The IUPAC Compendium of Chemical Terminology*. (International Union of Pure and Applied Chemistry (IUPAC), 2019).

29. Guarnieri, M. The Age of Vacuum Tubes: Early Devices and the Rise of Radio Communications [Historical]. *IEEE Ind. Electron. Mag.* **6**, 41-43 (2012).

30. Bizony, P. Smart Apollo [on-board Apollo guidance computer]. *Eng. Technol.* **4**, 59-61 (2009).

31. https://frankcomputerscience.wordpress.com/chapter-3/ (5.5.2021).

32. Dueñas-Díez, M. & Pérez-Mercader, J. How Chemistry Computes: Language Recognition by Non-Biochemical Chemical Automata. From Finite Automata to Turing Machines. *iScience* **19**, 514-526 (2019).

33. Unger-Angel, L., Motiei, L. & Margulies, D. Molecular Logic as a Means to Assess Therapeutic Antidotes. *Front. Chem.* **7**, (2019).

34. Fan, K., Yang, J., Wang, X. & Song, J. Rational construction of gel-based supramolecular logic gates by using a functional gelator with multiple-stimuli responsive properties. *Soft Matter* **10**, 8370-8375 (2014).

35. https://www.nobelprize.org/prizes/chemistry/1946/sumner/biographical/ (11.6.2021).

36. Hussain Qadri, S. M., Zubairi, S., Hawley, H. P., Mazlaghani, H. H. & Ramirez, E. G. Rapid test for determination of urea hydrolysis. *Antonie Van Leeuwenhoek* **50**, 417-423 (1984).

37. Konieczna, I. *et al.* Bacterial Urease and its Role in Long-Lasting Human Diseases. *Curr. Protein Pept. Sci.* **13**, 789-806 (2012).

38. Adams, F. & Barbante, C. Electron-Based Imaging Techniques. in 269-313 (2015).

39. Craievich, A. F. Small-Angle X-ray Scattering by Nanostructured Materials. in *Handbook of Sol-Gel Science and Technology* 1-46 (Springer International Publishing, 2016).

40. Liu, L., Boldon, L., Urquhart, M. & Wang, X. Small and Wide Angle X-Ray Scattering Studies of Biological Macromolecules in Solution. *J. Vis. Exp.* (2013).

41. Overview of AFM. in *Atomic Force Microscopy* 1-32 (John Wiley & Sons, Inc., 2012).

42. Li, J.-L., Liu, X.-Y., Wang, R.-Y. & Xiong, J.-Y. Architecture of a Biocompatible Supramolecular Material by Supersaturation-Driven Fabrication of its Fiber Network. *J. Phys. Chem. B* **109**, 24231-24235 (2005).

43. Eldridge, J. E. & Ferry, J. D. Studies of the Cross-linking Process in Gelatin Gels. III. Dependence of Melting Point on Concentration and Molecular Weight. *J. Phys. Chem.* **58**, 992-995 (1954).

44. Murata, K. *et al.* Thermal and Light Control of the Sol-Gel Phase Transition in Cholesterol-Based Organic Gels. Novel Helical Aggregation Modes As Detected by Circular Dichroism and Electron Microscopic Observation. *J. Am. Chem. Soc.* **116**, 6664-6676 (1994).

45. Alhalaweh, A., Alzghoul, A. & Bergström, C. A. S. Molecular Drivers of Crystallization Kinetics for Drugs in Supersaturated Aqueous Solutions. *J. Pharm. Sci.* **108**, 252-259 (2019).

46. Raina, S. A. *et al.* Trends in the Precipitation and Crystallization Behavior of Supersaturated Aqueous Solutions of Poorly Water-Soluble Drugs Assessed Using Synchrotron Radiation. *J. Pharm. Sci.* **104**, 1981-1992 (2015).

47. Schall, J. M., Capellades, G. & Myerson, A. S. Methods for estimating supersaturation in antisolvent crystallization systems. *CrystEngComm* **21**, 5811-5817 (2019).

48. Winter, H. H. Can the gel point of a cross-linking polymer be detected by theG′ -G′′ crossover? *Polym. Eng. Sci.* **27**, 1698-1702 (1987).

49. Adamczyk-Woźniak, A. *et al.* Dehydration of ortho -, meta - and para -Alkoxy Phenylboronic Acids to their Corresponding Boroxines. *Eur. J. Inorg. Chem.* **2018**, 1492-1498 (2018).

50. Qi, Z. *et al.* Systems chemistry: logic gates based on the stimuli-responsive gel-sol transition of a crown ether-functionalized bis(urea) gelator. *Chem. Sci.* **3**, 2073 (2012).

51. Brahimi-Horn, M. C. & Pouysségur, J. Hypoxia in cancer cell metabolism and pH regulation. *Essays Biochem.* **43**, 165-178 (2007).

52. O_Rourke, F. J. Formic Acid Production among the Formicidae. *Ann. Entomol. Soc. Am.* **43**, 437-443 (1950).

53. Zhong, M., Teng, Y., Pang, S., Yan, L. & Kan, X. Pyrrole-phenylboronic acid: A novel

monomer for dopamine recognition and detection based on imprinted electrochemical sensor. *Biosens. Bioelectron.* **64**, 212-218 (2015).

54. Pasparakis, G., Vamvakaki, M., Krasnogor, N. & Alexander, C. Diol-boronic acid complexes integrated by responsive polymers—a route to chemical sensing and logic operations. *Soft Matter* **5**, 3839 (2009).

55. Xue, P., Ding, J., Jin, M. & Lu, R. Rapid gel-to-sol transition triggered by a photoacid generator under low-power light. *J. Mater. Chem. C* **5**, 5299-5303 (2017).

56. Li, R.-J., Pezzato, C., Berton, C. & Severin, K. Light-induced assembly and disassembly of polymers with Pd n L 2n -type network junctions. *Chem. Sci.* **12**, 4981-4984 (2021).

57. Uotani, T. & Graham, D. Y. Diagnosis of Helicobacter pylori using the rapid urease test. *Ann. Transl. Med.* **3**, 9 (2015).

58. Katz, E. Enzyme-Based Logic Gates and Networks with Output Signals Analyzed by Various Methods. *ChemPhysChem* **18**, 1688-1713 (2017).